International Journal of Non-Linear Mechanics 46 (2011) 1177–1190

Contents lists available at ScienceDirect

International Journal of Non-Linear Mechanics

journal homepage: www.elsevier.com/locate/nlm

Double impact periodic orbits for an inverted pendulum ☆

Jun Shen, Zhengdong Du *

Department of Mathematics, Sichuan University Chengdu, Sichuan 610064, PR China

ARTICLE INFO

Article history:
Received 9 February 2011
Accepted 10 May 2011
Available online 27 May 2011

Keywords:
Impact inverted pendulum
Double impact periodic orbit
Grazing bifurcation
Piecewise linear system
Chaos

ABSTRACT

There exist many types of possible periodic orbits that impact at the walls for the inverted pendulum impacting between two rigid walls. Previous studies only focused on single impact periodic orbits and symmetric periodic orbits that bounce back and forth between the two walls. They respectively correspond to Types I and II orbits in the Chow, Shaw and Rand classification. In this paper we discuss two types of double impact periodic orbits that have not been studied before. The equations need to be solved for double impact orbits are transcendental and it is very hard to see the structure of the solutions. Consequently the analysis of double impact orbits is much more difficult than that of Types I and II orbits. A combination of analytical and numerical methods is employed to investigate the existence, stability and bifurcations of these orbits. Grazing bifurcations, which do not present for Types I and II orbits, are also observed.

1. Introduction

An impact system, where a vibrator collides with one or more rigid walls or with another moving object, is found in many applications, such as impact print hammers [14], rigid blocks [15] and walking machines [16], etc. Being an important class of piecewise smooth (PWS) dynamical systems, impact systems often exhibit very complicated dynamics. Besides the occurrence of all kinds of traditional bifurcations, such as saddle–node bifurcation, Hopf bifurcation as well as homoclinic bifurcation, period doubling bifurcation [5,32–34], impacts also lead to many new types of complicated bifurcation phenomena, such as grazing, sticking and chattering [3,4,6–8,11,27–29,35,36], etc. In general, such kinds of non-standard bifurcations arising from impact systems and other types of PWS systems are difficult to deal with because of the added non-linearities caused by the non-smoothness. In recent decades, the study of those non-standard bifurcations has become very active and some effective general methods have been developed. For instance, normal form calculations for impact oscillators were studied in [1,12] and a general methodology of reducing multidimensional flows to low-dimensional maps for piecewise non-linear oscillators was proposed in [30]. The characteristic of normal form map for soft impact systems was also analyzed in [26]. In fact there is an enormous literature on this subject, in addition to the aforementioned works, see, for example, the monographs [2,20] and the references therein for more on these issues.

In this paper we consider double impact periodic motions (namely, motions which repeat after every second impact) of the inverted pendulum impacting on rigid walls under external periodic excitation as shown in Fig. 1. We can scale the gap size between the two walls to be two and assume that the mathematical model is given by the following piecewise linear (PWL) differential equation:

$$\begin{cases} \ddot{x}+2\alpha\dot{x}-x=\beta\cos\omega t, & \text{as } |x|<1, \\ \dot{x}\mapsto -r\dot{x}, & \text{as } |x|=1, \end{cases} \tag{1.1}$$

where $\alpha>0$ is a linear damping coefficient and $\beta>0$ is the forcing amplitude, $r\in(0,1]$ is the coefficient of restitution representing energy loss during impact.

The PWL system (1.1) was first proposed by Chow and Shaw in [5] and also by Shaw and Rand in [34]. The subharmonic and homoclinic bifurcations and chaos were discussed for (1.1) in [5,34]. The impact inverted pendulum can be used in the modeling of many mechanical devices, such as rings, rigid standing structures, a mooring buoy, etc. [8]. Due to this reason, it has been extensively studied during the last 20 years. The existence and stability of periodic motions were analyzed under impulsive excitation in [23] and under general periodic excitation in [24]. Properties of cross-well chaos were studied in [32] and the problem of chaos control was addressed in [21,22]. The asymptotic analysis of chattering oscillations is presented in [8]. All of these works assume that the motion of the oscillator between the walls is governed by a linear equation. Efforts were also made in [9,10,25] to extend the Melnikov methods for homoclinic and subharmonic bifurcations established for smooth systems to the

☆ Supported by the MOE Fundamental Research Funds for the Central Universities (China) 2010SCU21005.

* Corresponding author.
E-mail address: zdu85@yahoo.com (Z. Du).

0020-7462/$ - see front matter © 2011 Elsevier Ltd. All rights reserved.
doi:10.1016/j.ijnonlinmec.2011.05.010

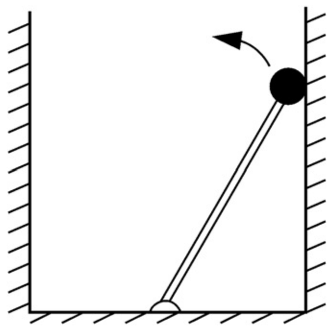

Fig. 1. Inverted pendulum.

impact inverted pendulum when the motion of the oscillator between the walls is governed by a general non-linear equation.

For the PWL system (1.1), there are many types of possible periodic motions involving impacts at $x=+1$ and -1. Let $T=2\pi/\omega$ be the period of the excitation. Let m be a positive integer and the triple (m,k_1,k_2) denote the periodic orbits of period mT of (1.1) that impact at $x=+1$ k_1 times and -1 k_2 times per period. Clearly, the $(m, 1, 0)$ and $(m, 0, 1)$ motions correspond to the Type I motions and the symmetrical $(m, 1, 1)$ motions correspond to the Type II motions in the classification given by Chow, Shaw and Rand in [5,34]. These two types of motions are the simplest forms of motions of (1.1) and have been thoroughly investigated by previous works mentioned above. As pointed out by Lenci and Rega [24], although in principle, the more general (m,k_1,k_2) periodic motions can be studied analytically, the formulation becomes rapidly cumbersome and the computations are extremely difficult for periodic motions impacting multiple times in their period. Consequently, to the best of our knowledge, for system (1.1) there is still no result on the study of periodic motions impacting two or more times in their period except for the symmetrical $(m, 1, 1)$ motions in the literature. It is worth noting that in [3], Budd and Lee studied the double impact periodic orbits of a class of periodically forced harmonic impact oscillators.

For system (1.1), there are two types of double impact periodic orbits. The first type is the $(m, 2, 0)$ (or $(m, 0, 2)$) motions. Namely, the pendulum starting from the wall $x=+1$ (or $x=-1$) immediately changes its velocity by the impact law and impact to $x=+1$ (or $x=-1$) after traveling for a time μmT for $\mu\in(0,1)$ without touching the walls $x=\pm 1$, then bounces back to $x=+1$ (or $x=-1$) after traveling for a time $(1-\mu)mT$ without touching the walls $x=\pm 1$, then repeat the above motion. In order to emphasis the distribution of the traveling times between each consecutive impacts, we denote the motions as $(m,2,0,\mu)$ or $(m,0,2,\mu)$ motions. By symmetry, for this type of double impact periodic orbits, we only need to study the $(m,2,0,\mu)$ motions. The second type is the $(m, 1, 1)$ motions. For this type of motions, the pendulum starting from the wall $x=+1$ immediately changes its velocity by the impact law and reaches the wall $x=-1$ after a time μmT for $\mu\in(0,1)$, and then bounces back to the wall $x=+1$ after traveling for another time of $(1-\mu)mT$ without touching the walls $x=\pm 1$, then repeat the above motion. We similarly denote this type of motions as $(m,1,1,\mu)$ motions. Clearly, when $\mu=\frac{1}{2}$, a $(m,2,0,\mu)$ (or $(m,0,2,\mu)$) orbit is reduced to a single impact periodic orbit. In fact, a $(m,2,0,\frac{1}{2})$ (or $(m,0,2,\frac{1}{2})$) orbit for even m and a $(m,1,1,\frac{1}{2})$ orbit are respectively a Type I orbit and a Type II orbit studied in [5,34]. Hence in this paper, we assume that $\mu\neq\frac{1}{2}$.

As shown in the sequel, unlike for a Type I orbit and a Type II orbit studied in [5,34], the equations need to be solved for double impact orbits are transcendental and it is very hard to see the structure of the solutions. Thus double impact orbits are much more difficult to analyze. A combination of analytical and numerical methods are used to investigate the existence, stability and bifurcations of these orbits in detail. Grazing bifurcations, which do not present for Types I and II orbits, are also observed.

This paper is organized as follows. In Section 2, we discuss the existence of the aforementioned two types of double impact periodic orbits. In Section 3, we discuss the double impact periodic orbits for some special cases. The stability and bifurcations of these orbits are given in Section 4. In Section 5, we present analytical conditions for the existence of double impact grazing periodic orbits. The grazing bifurcations are discussed in Section 6. Finally, some concluding remarks are given in Section 7.

2. The existence of double impact periodic orbits

Let $\dot{x}=y$, then the free motion between the two walls of PWL system (1.1) can be rewritten in the form:

$$\left.\begin{aligned}&\dot{x}=y\\&\dot{y}=x-2\alpha y+\beta\cos\omega\varphi\\&\dot{\varphi}=1\end{aligned}\right\}\quad \text{as } |x|<1, \tag{2.1}$$

where $\varphi=t(\text{mod}T)$ and $T=2\pi/\omega$ is the period of the excitation. The impact law is given by

$$y\to -ry\quad \text{as } |x|=1. \tag{2.2}$$

Let $\Omega=\sqrt{1+\alpha^2}$, $\gamma=\beta/q$, $q=\sqrt{(1+\omega^2)^2+4\alpha^2\omega^2}$. Then the solution of (2.1) corresponding to the initial conditions $x=x_0$, $y=y_0$, $\varphi=\varphi_0$ is given by

$$\begin{cases} x(t;x_0,y_0,\varphi_0)=e^{-\alpha(t-\varphi_0)}[C_1\cosh\Omega(t-\varphi_0)+C_2\sinh\Omega(t-\varphi_0)]\\ \qquad\qquad +\gamma\cos(\omega t+\psi),\\ y(t;x_0,y_0,\varphi_0)=e^{-\alpha(t-\varphi_0)}[(-\alpha C_1+\Omega C_2)\cosh\Omega(t-\varphi_0)\\ \qquad\qquad +(\Omega C_1-\alpha C_2)\sinh\Omega(t-\varphi_0)]-\gamma\omega\sin(\omega t+\psi),\end{cases} \tag{2.3}$$

where $\psi=\arctan(2\alpha\omega/(1+\omega^2))-\pi\in[-\pi,-\pi/2]$, C_1, C_2 are given by

$$C_1=x_0-\gamma\cos(\omega\varphi_0+\psi),\quad C_2=\frac{1}{\Omega}[\alpha C_1+y_0+\gamma\omega\sin(\omega\varphi_0+\psi)].$$

Because of the nature of the vector field (2.1) and (2.2), the Poincaré section is taken to be the cylinder:

$$\Sigma:=\{(\varphi,x,y)\in S^1\times I\times\mathbb{R}|x=1,y>0\}=S^1\times\mathbb{R}^+,$$

where $I:=[-1,1]$ and S^1 is the circle of period T. Let

$$\Sigma_-^+:=\{(\varphi,x,y)\in S^1\times I\times\mathbb{R}|x=1,y<0\},$$

$$\Sigma_+^-:=\{(\varphi,x,y)\in S^1\times I\times\mathbb{R}|x=-1,y>0\},$$

$$\Sigma_-^-:=\{(\varphi,x,y)\in S^1\times I\times\mathbb{R}|x=-1,y<0\}$$

be the other three half switch planes. Elements in Σ are denoted by $(\varphi,y)\in S^1\times\mathbb{R}^+$ and elements in Σ_-^+, Σ_+^- and Σ_-^- are still denoted by (φ,x,y) with $x=1$, -1 and $x=-1$ respectively. The Poincaré map $\Pi:\Sigma\mapsto\Sigma$ is given by the flow of systems (2.1) and (2.2).

Let m be a positive integer and $\mu\in(0,1)$ and $\mu\neq\frac{1}{2}$. Similar to [5,34], the conditions for the existence of a $(m,2,0,\mu)$ orbit are given below in terms of $(\varphi_m,y_m)\in\Sigma$:

$$x(\varphi_m+\mu mT;+1,-ry_m,\varphi_m)=+1, \tag{2.4a}$$

$$x(\varphi_m+mT;+1,-r\tilde{y}_{m,A},\varphi_m+\mu mT)=+1, \tag{2.4b}$$

$$y(\varphi_m+mT;+1,-r\tilde{y}_{m,A},\varphi_m+\mu mT)=y_m, \tag{2.4c}$$

$$|x(\varphi_m+t;+1,-ry_m,\varphi_m)|<1,\quad t\in(0,\mu mT), \tag{2.4d}$$

$$|x(\varphi_m+\mu mT+t;+1,-r\tilde{y}_{m,A},\varphi_m+\mu mT)|<1,\quad t\in(0,(1-\mu)mT), \tag{2.4e}$$

where $\tilde{y}_{m,A} = y(\varphi_m + \mu mT; +1, -ry_m, \varphi_m)$. Similarly, the conditions for the existence of a $(m,1,1,\mu)$ motion are given below in terms of $(\varphi_m, y_m) \in \Sigma$:

$$x(\varphi_m + \mu mT; +1, -ry_m, \varphi_m) = -1, \tag{2.5a}$$

$$x(\varphi_m + mT; -1, -r\tilde{y}_{m,B}, \varphi_m + \mu mT) = +1, \tag{2.5b}$$

$$y(\varphi_m + mT; -1, -r\tilde{y}_{m,B}, \varphi_m + \mu mT) = y_m, \tag{2.5c}$$

$$|x(\varphi_m + t; +1, -ry_m, \varphi_m)| < 1, \quad t \in (0, \mu mT), \tag{2.5d}$$

$$|x(\varphi_m + \mu mT + t; -1, -r\tilde{y}_{m,B}, \varphi_m + \mu mT)| < 1, \quad t \in (0, (1-\mu)mT), \tag{2.5e}$$

where $\tilde{y}_{m,B} = y(\varphi_m + \mu mT; +1, -ry_m, \varphi_m)$. When $\tilde{y}_{m,A} = 0$ (resp. $\tilde{y}_{m,B} = 0$), the corresponding $(m,2,0,\mu)$ (resp. $(m,1,1,\mu)$) orbit is a grazing periodic orbit, which will be discussed in detail in Sections 5 and 6.

To simplify expressions in the sequel, we introduce the following notations:

$$G(\mu) = (e^{\alpha\mu mT} + re^{-\alpha\mu mT})\sinh((1-\mu)mT\Omega),$$

$$H(\mu) = 2\omega(1+r)\Omega(G(\mu) - G(1-\mu)),$$

$$I = \cosh(mT\Omega) - \cosh(\alpha mT),$$

$$J = (1-r)I + (1+r)\left(\frac{\alpha}{\Omega}\sinh(mT\Omega) - \sinh(\alpha mT)\right),$$

$$K_\pm(\mu) = (1+r)[2\alpha\sinh(\mu mT\Omega)\sinh((1-\mu)mT\Omega) \pm \Omega\sinh((1-2\mu)mT\Omega)] + (1-r)\Omega\sinh(mT\Omega),$$

$$L(\mu) = 2\Omega e^{\alpha\mu mT}[\sinh((1-\mu)mT\Omega) - re^{-\alpha mT}\sinh(\mu mT\Omega)],$$

$$M_\pm(\mu) = (1+r)\omega[-K_+(\mu) \pm L(\mu)],$$

$$N_\pm(\mu) = (1+r)\omega[\pm K_-(\mu) - L(1-\mu)],$$

$$Q(\mu) = e^{-\alpha mT}\sinh(\mu mT\Omega) + \sinh((1-\mu)mT\Omega),$$

$$R(\mu) = e^{-\alpha mT}\cosh(\mu mT\Omega) - \cosh((1-\mu)mT\Omega),$$

$$S_\pm(\mu) = \Omega J \pm (1+r)e^{\alpha\mu mT}[\alpha Q(\mu) + \Omega R(\mu)],$$

$$U(\mu) = -[(1-r)^2 + 2\alpha^2(1+r^2)]\cosh(mT\Omega) - (1+r)^2\cosh((1-2\mu)mT\Omega) - 2\alpha\Omega(1-r^2)\sinh(mT\Omega) + 2\Omega^2(e^{\alpha mT} + r^2e^{-\alpha mT}),$$

$$\Delta(\mu) = \{U(\mu) - \omega^2(1+r)^2[\cosh(mT\Omega) - \cosh((1-2\mu)mT\Omega)]\}\sin(2\mu m\pi) - 2\omega\Omega(1+r)^2\sinh((1-2\mu)mT\Omega)\cos(2\mu m\pi) + H(\mu),$$

$$\Delta_1^\pm(\mu) = U(\mu)\sin(2\mu m\pi) + M_\pm(\mu)\cos(2\mu m\pi) + N_\pm(\mu),$$

$$\Delta_2^\pm(\mu) = -M_\pm(\mu)\sin(2\mu m\pi) + U(\mu)\cos(2\mu m\pi) \mp U(\mu),$$

$$\Delta_3^\pm(\mu) = \pm 2\omega^2\Omega(1+r)[e^{\alpha\mu mT}Q(\mu) \mp \sinh(mT\Omega)]\sin(2\mu m\pi) + 2\omega\Omega S_\pm(\mu)\cos(2\mu m\pi) \mp 2\omega\Omega S_\pm(\mu).$$

Then the main result of this section is as follows:

Theorem 2.1. *Let m be a positive integer and $\mu \in (0,1)$ and $\mu \neq \frac{1}{2}$. Let $c_m = \cos(\omega\varphi_m + \psi)$, $s_m = \sin(\omega\varphi_m + \psi)$. Then for system* (1.1):

(1) *A point $(\varphi_m, y_m) \in \Sigma$ is a period-2 point of Π and corresponds to a $(m,2,0,\mu)$ orbit if and only if* (2.4d) *and* (2.4e) *holds and the following are satisfied*:

$$\Delta(\mu) \neq 0, \quad c_m = \frac{\Delta_1^+(\mu)}{\gamma\Delta(\mu)}, \quad s_m = \frac{\Delta_2^+(\mu)}{\gamma\Delta(\mu)},$$

$$y_m = \frac{\Delta_3^+(\mu)}{\Delta(\mu)}, \quad \gamma = \frac{\sqrt{\Delta_1^+(\mu)^2 + \Delta_2^+(\mu)^2}}{|\Delta(\mu)|}.$$

(2) *A point $(\varphi_m, y_m) \in \Sigma$ is a fixed point of Π and corresponds to a $(m,1,1,\mu)$ orbit if and only if* (2.5d) *and* (2.5e) *holds and the following are satisfied*:

$$\Delta(\mu) \neq 0, \quad c_m = \frac{\Delta_1^-(\mu)}{\gamma\Delta(\mu)}, \quad s_m = \frac{\Delta_2^-(\mu)}{\gamma\Delta(\mu)},$$

$$y_m = \frac{\Delta_3^-(\mu)}{\Delta(\mu)}, \quad \gamma = \frac{\sqrt{\Delta_1^-(\mu)^2 + \Delta_2^-(\mu)^2}}{|\Delta(\mu)|}.$$

To prove Theorem 2.1, we need the following result.

Lemma 2.1. *For $\mu \in (0,1)$ and $\mu \neq \frac{1}{2}$, $M_\pm(\mu) \pm N_\pm(\mu) \neq 0$ and $U(\mu) \neq 0$.*

Proof. We only prove $M_+(\mu) \pm N_+(\mu) \neq 0$ and $U(\mu) \neq 0$. The proof for $M_-(\mu) \pm N_-(\mu) \neq 0$ is similar to that of $M_+(\mu) \pm N_+(\mu) \neq 0$.

Let $g_1(\tau) = \cosh(\tau\mu mT)$, $g_2(\tau) = \cosh(\tau(1-\mu)mT)$ and

$$g_3(\tau) = (1-r)\sinh(\mu mT\Omega)\sinh((1-\mu)mT\Omega)\frac{\sinh(\tau\alpha mT)}{\sinh(\tau mT\Omega)},$$

$$g_4(\tau) = \frac{(1+r)\Xi\sinh(\tau mT\Omega)}{\cosh(\tau mT\Omega) - \cosh(\tau\alpha mT)},$$

where $\Xi = [g_1(\Omega) - g_1(\alpha)][g_2(\Omega) - g_2(\alpha)] > 0$. Then $g_3(\tau)$ and $g_4(\tau)$ are both strictly decreasing for $\tau > 0$. Thus for $\mu \in (0,1)$ and $\mu \neq \frac{1}{2}$, we have

$$M_+(\mu) + N_+(\mu) = 2(1+r)\omega\Omega\sum_{k=3}^{4}(g_k(\mu) - g_k(1-\mu)) \neq 0.$$

Let

$$h_1(\tau) = (1-r)\frac{\cosh(\tau\mu mT)}{\sinh(\mu mT\Omega)} + \alpha(1+r)\frac{\sinh(\tau\mu mT)}{\tau\sinh(\mu mT\Omega)},$$

$$h_2(\tau) = (1-r)\frac{\cosh(\tau(1-\mu)mT)}{\sinh((1-\mu)mT\Omega)} + \alpha(1+r)\frac{\sinh(\tau(1-\mu)mT)}{\tau\sinh((1-\mu)mT\Omega)}.$$

Then $h_1(\tau)$ and $h_2(\tau)$ are both strictly increasing for $\tau > 0$. Note that $M_+(\mu) - N_+(\mu) = 2(1+r)\omega\Omega\Theta$, where

$$\Theta = \sinh(\mu mT\Omega)\sinh((1-\mu)mT\Omega)\sum_{k=1}^{2}(h_k(\alpha) - h_k(\Omega)).$$

Hence $M_+(\mu) - N_+(\mu) < 0$ because $\alpha < \Omega = \sqrt{1+\alpha^2}$.

Finally, it is obvious that $U(\mu)$ reaches its maximum at $\mu = \frac{1}{2}$ for $\mu \in (0,1)$. Thus for $\mu \neq \frac{1}{2}$, we have $U(\mu) < U(\frac{1}{2}) < 0$. The proof is complete. □

Proof of Theorem 2.1. We only prove (1), the proof for (2) is similar.

From (2.3), we obtain

$$\tilde{y}_{m,A} = \tilde{y}_{m,B} = -\gamma[\Lambda(\mu) + \omega\sin(2\mu m\pi)]c_m - \omega\gamma[\Gamma(\mu) + \cos(2\mu m\pi)]s_m + r\Gamma(\mu)y_m + \Lambda(\mu), \tag{2.6}$$

where

$$\Lambda(\mu) = \frac{1}{\Omega}e^{-\alpha\mu mT}\sinh(\mu mT\Omega), \quad \Gamma(\mu) = \alpha\Lambda(\mu) - e^{-\alpha\mu mT}\cosh(\mu mT\Omega).$$

Substitute (2.3) and (2.6) into (2.4a)–(2.4c), we obtain a system of linear equations for c_m, s_m and y_m of the form:

$$\mathbf{a}_1(\mu)c_m + \mathbf{a}_2(\mu)s_m + \mathbf{a}_3(\mu)y_m = \mathbf{b}(\mu), \tag{2.7}$$

where $\mathbf{a}_1(\mu), \mathbf{a}_2(\mu), \mathbf{a}_3(\mu), \mathbf{b}(\mu) \in \mathbb{R}^3$ are column vectors, their expressions are very complicated, and hence are omitted here for brevity. Let $\mathbf{A}(\mu)$ be the coefficient matrix of (2.7) and $\mathbf{A}_k(\mu)$ (k=1, 2, 3) be 3×3 matrices obtained by replacing the k-th column of $\mathbf{A}(\mu)$ with $\mathbf{b}(\mu)$. With Maple, we find that

$$\det\mathbf{A}(\mu) = \frac{\gamma^2}{2\Omega^2} e^{\alpha(1-\mu)mT}\Delta(\mu), \quad \det\mathbf{A}_1(\mu) = \frac{\gamma}{2\Omega^2} e^{\alpha(1-\mu)mT}\Delta_1^+(\mu),$$

$$\det\mathbf{A}_2(\mu) = \frac{\gamma}{2\Omega^2} e^{\alpha(1-\mu)mT}\Delta_2^+(\mu), \quad \det\mathbf{A}_3(\mu) = \frac{\gamma^2}{2\Omega^2} e^{\alpha(1-\mu)mT}\Delta_3^+(\mu).$$

If $\Delta(\mu) \neq 0$, then c_m, s_m and y_m can be solved from (2.7) using Cramer's rule. The condition for γ can be found from the identity $c_m^2 + s_m^2 = 1$.

We now prove that if $\Delta(\mu) = 0$, then (2.7) has no solution. Consequently, the $(m,2,0,\mu)$ orbit does not exist. In fact, if this is not true, then (2.7) has infinitely many solutions, implying that $\text{rank}(\mathbf{A}(\mu)) = \text{rank}(\mathbf{A}(\mu)\ \mathbf{b}(\mu)) \leq 2$. Thus $\Delta_1^+(\mu) = \Delta_2^+(\mu) = \Delta_3^+(\mu) = 0$. By Lemma 2.1, $U(\mu) \neq 0$. Hence from $\Delta_1^+(\mu) = \Delta_2^+(\mu) = 0$, we can uniquely solve for $\tilde{s}_m := \sin(2\mu m\pi)$, $\tilde{c}_m := \cos(2\mu m\pi)$:

$$\tilde{s}_m = -\frac{U(\mu)(M_+(\mu)+N_+(\mu))}{U(\mu)^2 + M_+(\mu)^2}, \quad \tilde{c}_m = 1 - \frac{M_+(\mu)(M_+(\mu)+N_+(\mu))}{U(\mu)^2 + M_+(\mu)^2}.$$

However, from $\tilde{s}_m^2 + \tilde{c}_m^2 = 1$ we get $(M_+(\mu)+N_+(\mu))(M_+(\mu) - N_+(\mu)) = 0$, which is a contradiction to Lemma 2.1. The proof of Theorem 2.1 is complete. $\square$

By Theorem 2.1 and (2.3), we can obtain the following result:

Corollary 2.1. *A $(m,2,0,\mu)$ orbit coexists with a $(m,2,0,1-\mu)$ orbit and they overlap. A $(m,1,1,\mu)$ orbit coexists with a $(m,1,1,1-\mu)$ orbit and they are symmetric with respect to the origin.*

Remark 2.1. It is easy to prove that $\Delta(\frac{1}{2}) = 0$. If m is odd, then $\Delta_2^+(\frac{1}{2}) = -2U(\frac{1}{2}) \neq 0$, implying that a $(m,2,0,\frac{1}{2})$ orbit does not exist. If m is even, a $(m,2,0,\frac{1}{2})$ orbit is simply a Type I orbit studied in [5,34]. Similarly, if m is odd, a $(m,1,1,\frac{1}{2})$ orbit is a Type II orbit studied in [5,34] and if m is even, a $(m,1,1,\frac{1}{2})$ orbit does not exist.

Clearly, to apply Theorem 2.1 to obtain a double impact periodic orbit of system (1.1), we need to verify the condition $\Delta(\mu) \neq 0$. Since $\Delta(\mu)$ is a complicated transcendental function, it is impossible to analytically find all zeros of $\Delta(\mu)$ and we must use numerical methods such as Newton's iterative method for this purpose. Consequently, it is impossible to analytically get all double impact periodic orbits of system (1.1). However, we have the following partial result:

Proposition 2.1. *Let m be a positive integer. If m=2p is an even number and*

$$\mu \in \mathcal{F}_A := \left(\bigcup_{k=0}^{p-1}\left[\frac{2k+1}{2m}, \frac{k+1}{m}\right]\right) \bigcup \left(\bigcup_{k=p}^{2p-1}\left[\frac{k}{m}, \frac{2k+1}{2m}\right]\right) - \left\{\frac{1}{2}\right\},$$

or if $m = 2p+1$ is an odd number and

$$\mu \in \mathcal{F}_B := \left(\bigcup_{k=0}^{p-1}\left[\frac{2k+1}{2m}, \frac{k+1}{m}\right]\right) \bigcup \left(\bigcup_{k=p+1}^{2p}\left[\frac{k}{m}, \frac{2k+1}{2m}\right]\right),$$

then $\Delta(\mu) \neq 0$.

Proof. Since $\Delta(1-\mu) = -\Delta(\mu)$, we only need consider this problem for $\mu \in (0, \frac{1}{2})$. Let $\varrho(\mu) = U(\mu) - \omega^2(1+r)^2[\cosh(mT\Omega) - \cosh((1-2\mu)mT\Omega)]$. Then for $\omega \neq 1$, $\varrho'(\mu) = 0$ if and only if $\mu = \frac{1}{2}$ and for $\omega = 1$, $\varrho'(\mu) \equiv 0$. Thus for $\mu \in [0, \frac{1}{2}]$, $\varrho(\mu) \leq \max(\varrho(0), \varrho(\frac{1}{2}))$. It is elementary to prove that $\varrho(0) < 0$, $\varrho(\frac{1}{2}) < 0$. Hence for $\mu \in [0, \frac{1}{2}]$, $\varrho(\mu) < 0$.

Now let $\varpi(\mu) = \Delta(\mu) - \varrho(\mu)\sin(2\mu m\pi)$ and

$$\varpi_0(\mu) = -2\omega\Omega(1+r)^2\sinh((1-2\mu)mT\Omega) + H(\mu).$$

Then

$$\varpi_0(\mu) = 2(1+r)\omega\Omega\sinh(\mu mT\Omega)\sinh((1-\mu)mT\Omega)(\Upsilon(\mu) - \Upsilon(1-\mu)),$$

where

$$\Upsilon(\tau) = \frac{(1-r)\sinh(\tau\alpha mT) - (1+r)[\cosh(\tau mT\Omega) - \cosh(\tau\alpha mT)]}{\sinh(\tau mT\Omega)}.$$

It is easy to see that $\Upsilon(\tau)$ is strictly decreasing for $\tau > 0$. Thus for $\mu \in (0, \frac{1}{2})$, $\varpi_0(\mu) > 0$. Hence for $\mu \in (0, \frac{1}{2})$,

$$\varpi(\mu) = -2\omega\Omega(1+r)^2\sinh((1-2\mu)mT\Omega)\cos(2\mu m\pi) + H(\mu) \geq \varpi_0(\mu) > 0.$$

Thus, when m=2p is even and $\mu \in (0, \frac{1}{2}) \bigcap \mathcal{F}_A$, $\varrho(\mu) < 0$, $\sin(2\mu m\pi) \leq 0$ and $\varpi(\mu) > 0$, implying that $\Delta(\mu) = \varpi(\mu) + \varrho(\mu)\sin(2\mu m\pi) > 0$. By the same argument, when $m = 2p+1$ is odd, then we have $\Delta(\mu) > 0$ for $\mu \in (0, \frac{1}{2}) \bigcap \mathcal{F}_B$. The proof of Proposition 2.1 is complete. $\square$

With Maple we apply the above results to simulate two double impact periodic orbits of system (1.1). Take m=3, α=4, r=0.5, $\omega = 16\pi$. In order to simulate a (3,2,0,0.252) orbit and a (3,2,0,0.748) orbit, we substitute these data into Theorem 2.1(1) and obtain $\beta \approx 6.0964759$. For the (3,2,0,0.252) orbit, $\varphi_m \approx 0.06175778951$ and $y_m \approx 0.07481707689$. For the (3,2,0,0.748) orbit, $\varphi_m \approx 0.03125778948$ and $y_m \approx 0.1736134324$. By the results on stability analysis given in section 3, it is not difficult to prove that

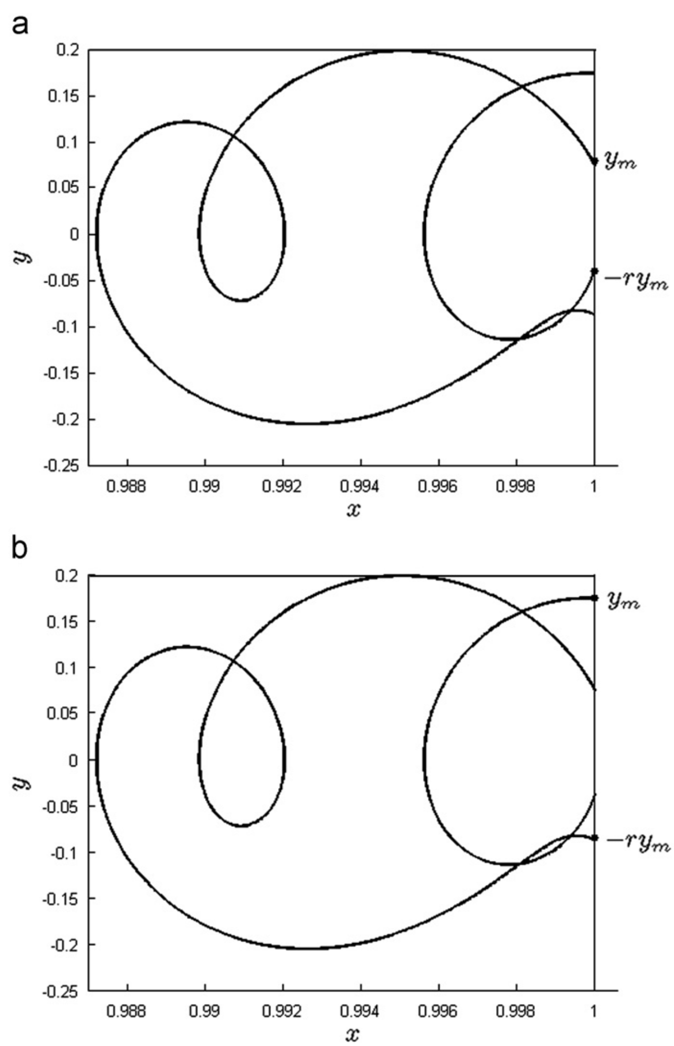

Fig. 2. (a) A (3, 2, 0, 0.252) orbit, (b) a (3, 2, 0, 0.748) orbit with m=3, α=4, r=0.5, ω=16π.

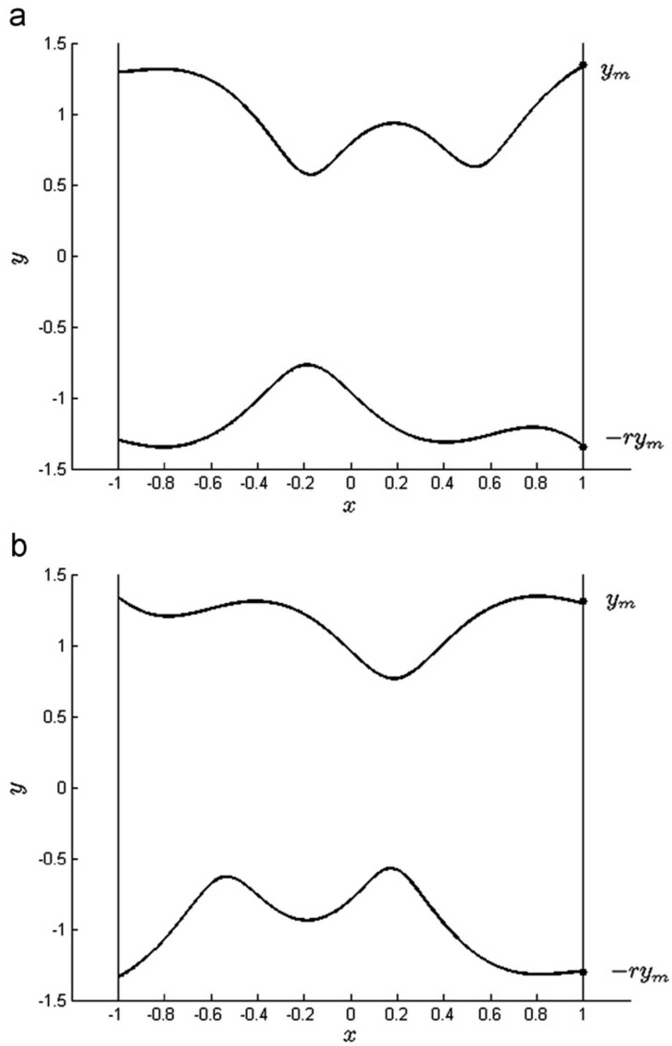

Fig. 3. (a) A (4, 1, 1, 0.442) orbit, (b) a (4, 1, 1, 0.558) orbit with m=4, $\alpha=\frac{1}{13}$, r=1, $\omega=2\pi$.

the resulted (3,2,0,0.252) orbit and (3,2,0,0.748) orbit are stable. The result is shown in Fig. 2. It is clear from Fig. 2 that the two orbits overlap. Similarly, take m=4, $\alpha=\frac{1}{13}$, r=1, $\omega=2\pi$, we obtain $\beta \approx 1.350303765$. For the (4,1,1,0.442) orbit, $\varphi_m \approx 0.2038771111$ and $y_m \approx 1.335757915$. For the (4,1,1,0.558) orbit, $\varphi_m \approx 0.4718771104$ and $y_m \approx 1.293757915$. With these data we simulate the stable (4,1,1,0.442) orbit and (4,1,1,0.558) orbit, which is shown in Fig. 3. It is clear from Fig. 3 that these two orbits are symmetric with respect to the origin.

3. Some special cases

As seen in Theorem 2.1, the analytical conditions for the existence of general double impact periodic orbits of system (1.1) are very complicated. In this section, we discuss some special cases, namely, the $(m,2,0,k/2m)$ orbits for odd k $(k \neq m)$ and the $(m,1,1,k/m)$ orbits for integer k $(k \neq m/2)$. We will give more concrete conditions for the existence of these orbits.

For $\sigma > 0$ and $\tau \in [0,1]$, we define two functions:

$$p(\sigma)=\Omega-2\alpha+e^{-2\sigma T\Omega}[\Omega+2\alpha+\Omega e^{\sigma(\Omega+\alpha)T}-3\Omega e^{\sigma(\Omega-\alpha)T}],$$

$$\psi(\tau)=(1+\tau)[\alpha\sinh(mT\Omega)-\Omega\sinh(\alpha mT)]-\tau I\Omega.$$

Obviously, $S_+(0)=2\psi(r)$, $\psi(0)>0$ and $\psi(1)=-\frac{1}{2}e^{mT\Omega}p(m)$. Furthermore, it is elementary to prove the following result.

Lemma 3.1. *For $\alpha \in (0,1/\sqrt{3}]$, $p(\sigma)>0$ when $\sigma>0$. For $\alpha>1/\sqrt{3}$, $p(\sigma)$ has a unique positive zero $\sigma_*>0$. Furthermore, $p(\sigma)>0$ when $\sigma \in (0,\sigma_*)$ and $p(\sigma)<0$ when $\sigma>\sigma_*$.*

By Lemma 3.1, it is easy to see that when $\alpha \in (0,1/\sqrt{3}]$, or $\alpha>1/\sqrt{3}$ and $1 \le m < \sigma_*$, $\psi(1)<0$, implying that $\psi(\tau)$ has a unique zero $r_* \in (0,1)$. When $\alpha>1/\sqrt{3}$ and $m \ge \sigma_*$, $\psi(1) \ge 0$, hence $\psi(\tau)>0$ for $\tau \in [0,1)$.

Lemma 3.2. *$S_-(\mu)$ is strictly decreasing for $\mu \in (0,1)$ and has a unique zero $\mu_*^- \in (0,1)$. Furthermore, $\mu_*^- \in (\frac{1}{2},1)$. $S_+(\mu)$ is strictly increasing for $\mu \in (0,1)$. When $\alpha \in (0,1/\sqrt{3}]$ and $r \in (0,r_*]$, or $\alpha>1/\sqrt{3}$, $1 \le m < \sigma_*$ and $r \in (0,r_*]$, or $\alpha>1/\sqrt{3}$ and $m \ge \sigma_*$, $S_+(\mu)>0$ for $\mu \in (0,1]$. When $\alpha \in (0,1/\sqrt{3}]$ and $r \in (r_*,1]$, or $\alpha>1/\sqrt{3}$, $1 \le m < \sigma_*$ and $r \in (r_*,1]$, $S_+(\mu)$ has a unique zero $\mu_*^+ \in (0,1)$. Furthermore, $\mu_*^+ \in (0,\frac{1}{2})$, $S_+(\mu)<0$ when $\mu \in (0,\mu_*^+)$ and $S_+(\mu)>0$ when $\mu \in (\mu_*^+,1)$.*

Proof. We only prove the statement for $S_+(\mu)$. The proof for $S_-(\mu)$ is similar and is actually easier.

It is easy to see that $S'_+(\mu)>0$ for $\mu \in (0,1)$, thus $S_+(\mu)$ is strictly increasing. Note that $S_+(0)=2\psi(r)$ and

$$S_+\left(\frac{1}{2}\right)=\Omega(1-r)I+2\alpha\Omega(1+r)\left[\cosh\left(\frac{mT\Omega}{2}\right)+\cosh\left(\frac{\alpha mT}{2}\right)\right] \times\left[\frac{1}{\Omega}\sinh\left(\frac{mT\Omega}{2}\right)-\frac{1}{\alpha}\sinh\left(\frac{\alpha mT}{2}\right)\right]>0,$$

since $\Omega>\alpha$. Due to the properties of $\psi(\tau)$ $(\tau \in [0,1])$ stated above, the assertions of Lemma 3.2 are true. Lemma 3.2 is thus proved. □

Moreover, from (2.6) we see that if a $(m,2,0,k/2m)$ orbit exists, then

$$y_m=-4\omega\Omega\frac{S_+\left(\frac{k}{2m}\right)}{\Delta\left(\frac{k}{2m}\right)}, \quad \tilde{y}_{m,A}=4\omega\Omega\frac{S_+\left(1-\frac{k}{2m}\right)}{\Delta\left(\frac{k}{2m}\right)}.$$

If a $(m,1,1,k/m)$ orbit exists, then

$$y_m=4\omega\Omega\frac{S_-\left(\frac{k}{m}\right)}{\Delta\left(\frac{k}{m}\right)}, \quad \tilde{y}_{m,B}=4\omega\Omega\frac{S_-\left(1-\frac{k}{m}\right)}{\Delta\left(\frac{k}{m}\right)}.$$

Thus, by Lemma 3.2 and Theorem 2.1, we obtain the following result.

Theorem 3.1. *Let $m>0$, $k>0$ be integers. Then for* (1.1):

(1) *If k is odd and a $(m,2,0,k/2m)$ orbit exists, then $k \in [1,2m\mu_*^+) \cup (2m(1-\mu_*^+),2m-1]$, $\alpha \in (0,1/\sqrt{3}]$ and $r \in (r_*,1]$, or $\alpha>1/\sqrt{3}$, $1 \le m < \sigma_*$ and $r \in (r_*,1]$. In this case, a point $(\varphi_m,y_m) \in \Sigma$ is a period-2 point of Π and corresponds to a $(m,2,0,k/2m)$ orbit if and only if* (2.4d) *and* (2.4e) *holds and the following are satisfied*:

$$c_m=\frac{\Delta_1^+\left(\frac{k}{2m}\right)}{\gamma\Delta\left(\frac{k}{2m}\right)}, \quad s_m=\frac{\Delta_2^+\left(\frac{k}{2m}\right)}{\gamma\Delta\left(\frac{k}{2m}\right)}, \quad y_m=\frac{\Delta_3^+\left(\frac{k}{2m}\right)}{\Delta\left(\frac{k}{2m}\right)},$$

$$\gamma=\frac{\sqrt{\Delta_1^+\left(\frac{k}{2m}\right)^2+\Delta_2^+\left(\frac{k}{2m}\right)^2}}{\left|\Delta\left(\frac{k}{2m}\right)\right|},$$

where $\Delta(k/2m)=2\omega\Omega(1+r)^2\sinh((m-k)T\Omega)+H(k/2m)$, $\Delta_1^+(k/2m)=-M_+(k/2m)+N_+(k/2m)$, $\Delta_2^+(k/2m)=-2U(k/2m)$, $\Delta_3^+(k/2m)=-4\omega\Omega S_+(k/2m)$.

(2) *If a* $(m,1,1,k/m)$ *orbit exists, then* $k\in[1,m(1-\mu_*^-))\cup(m\mu_*^-,m-1]$. *In this case, a point* $(\varphi_m,y_m)\in\Sigma$ *is a fixed point of* Π *and corresponds to a* $(m,1,1,k/m)$ *orbit if and only if* (2.5d) *and* (2.5e) *holds and the following are satisfied*:

$$c_m=\frac{\Delta_1^-\left(\frac{k}{m}\right)}{\gamma\Delta\left(\frac{k}{m}\right)},\quad s_m=\frac{\Delta_2^-\left(\frac{k}{m}\right)}{\gamma\Delta\left(\frac{k}{m}\right)},\quad y_m=\frac{\Delta_3^-\left(\frac{k}{m}\right)}{\Delta\left(\frac{k}{m}\right)},$$

$$\gamma=\frac{\sqrt{\Delta_1^-\left(\frac{k}{m}\right)^2+\Delta_2^-\left(\frac{k}{m}\right)^2}}{\left|\Delta\left(\frac{k}{m}\right)\right|},$$

where $\Delta(k/m)=-2\omega\Omega(1+r)^2\sinh((m-2k)T\Omega)+H(k/m)$, $\Delta_1^-(k/m)=M_-(k/m)+N_-(k/m)$, $\Delta_2^-(k/m)=2U(k/m)$, $\Delta_3^-(k/m)=4\omega\Omega S_-(k/m)$.

By Corollary 2.1, under the assumptions of Theorem 3.1, a $(m,2,0,k/2m)$ orbit coexists with a $(m,2,0,1-k/2m)$ orbit and they overlap; a $(m,1,1,k/m)$ orbit coexists with a $(m,1,1,1-k/m)$ orbit and they are symmetric with respect to the origin.

Remark 3.1. If k is even, then a $(m,2,0,k/2m)$ orbit does not exist. In fact, if this is not true, then by Theorem 2.1, we have $s_m=0$, $c_m=1$, $y_m=0$ and $\beta=q$, the corresponding orbit is given by $(x(t,+1,0,\varphi_m),y(t;+1,0,\varphi_m))=(\cos(\omega t+\psi),-\omega\sin(\omega t+\psi))$, but it is not of type $(m,2,0,\mu)$.

In Fig. 4, take $m=4$, $k=1$, $\alpha=1/\sqrt{3}$, $r=0.8$, $\omega=20$ and using the same method as described in Section 2, we simulate a $(4,2,0,\frac{1}{8})$ orbit (see Fig. 4(a)) and a $(4,2,0,\frac{7}{8})$ orbit (see Fig. 4(b)). For both orbits, we have $\beta\approx 8.025072$. For the $(4,2,0,\frac{1}{8})$ orbit, $\varphi_m\approx 0.1875739775$ and $y_m\approx 0.1365415013$. For the $(4,2,0,\frac{7}{8})$ orbit, $\varphi_m\approx 0.0304943449$ and $y_m\approx 0.5060179103$. It is clear from Fig. 4 that the two orbits overlap.

In Fig. 5, take $m=5$, $k=1$, $\alpha=\frac{1}{32}$, $r=1$, $\omega=\frac{5}{3}\pi$, we simulate a $(5,1,1,\frac{1}{5})$ orbit (see Fig. 5(a)) and a $(5,1,1,\frac{4}{5})$ orbit (see Fig. 5(b)). For both orbits, we have $\beta\approx 6.1614336$. For the $(5,1,1,\frac{1}{5})$ orbit, $\varphi_m\approx 0.07131158154$ and $y_m\approx 1.601727958$. For the $(5,1,1,\frac{4}{5})$ orbit, $\varphi_m\approx 0.6713115816$ and $y_m\approx 1.273692693$. It is clear from Fig. 5 that the two orbits are symmetric with respect to the origin.

4. Stability and bifurcation analysis

To determine the stability of the double impact periodic motions of system (1.1), we compute the eigenvalues of the Jacobian matrix $D\Pi$ of the corresponding Poincaré map $\Pi:\Sigma\mapsto\Sigma$. They are the solutions of the equation:

$$\lambda^2-\mathrm{Tr}(D\Pi)\lambda+\det(D\Pi)=0,$$

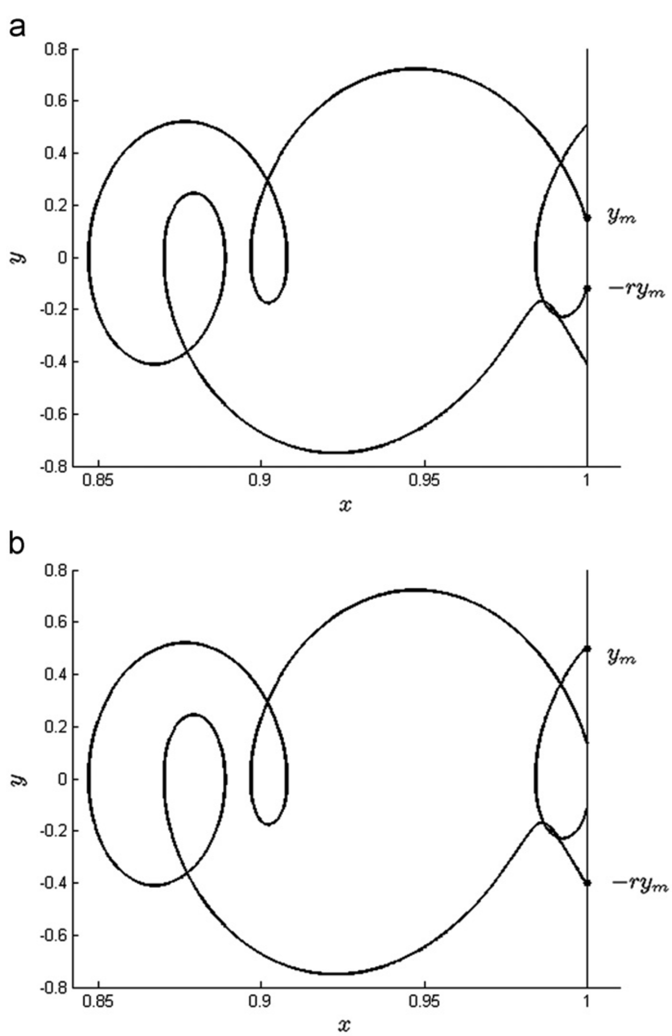

Fig. 4. (a) A $(4,2,0,\frac{1}{8})$ orbit, (b) a $(4,2,0,\frac{7}{8})$ orbit with $m=4$, $\alpha=1/\sqrt{3}$, $r=0.8$, $\omega=20$.

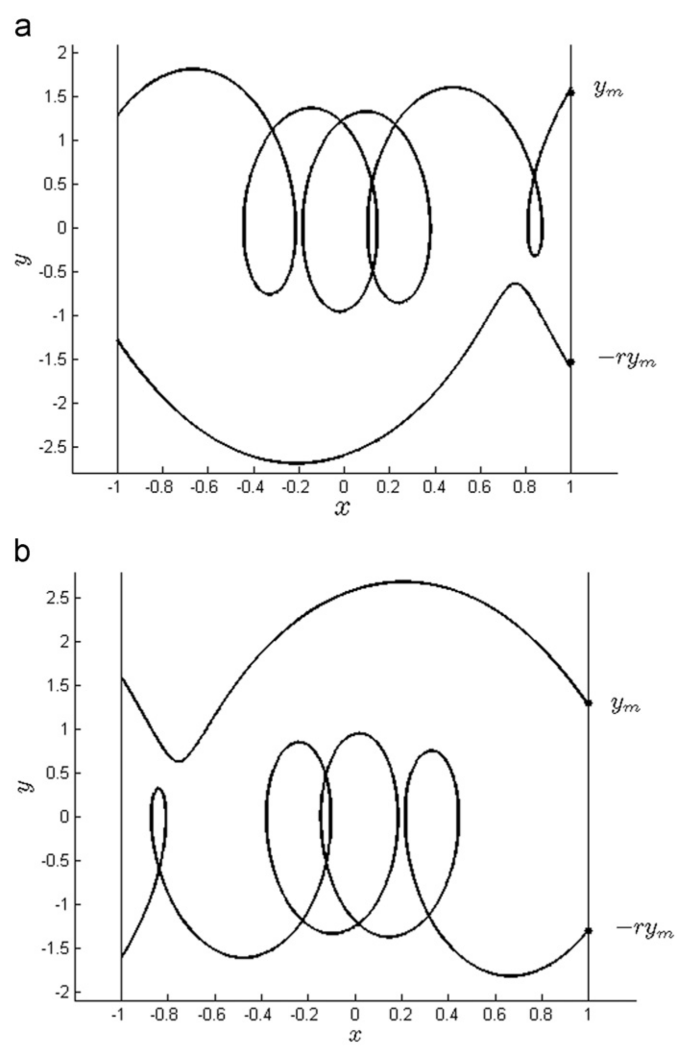

Fig. 5. (a) A $(5,1,1,\frac{1}{5})$ orbit, (b) a $(5,1,1,\frac{4}{5})$ orbit with $m=5$, $\alpha=\frac{1}{32}$, $r=1$, $\omega=\frac{5}{3}\pi$.

which are given by

$$\lambda_{1,2}=\frac{1}{2}\left[\mathrm{Tr}(D\Pi)\pm\sqrt{\mathrm{Tr}(D\Pi)^2-4\det(D\Pi)}\right], \tag{4.1}$$

where $\det(D\Pi)$ and $\mathrm{Tr}(D\Pi)$ are respectively the determinant and the trace of $D\Pi$. If $|\lambda_{1,2}|<1$, then the orbit is stable, if there exists a $|\lambda_k|>1$ (k=1 or 2), then the orbit is unstable.

Let $|\lambda_1|=\max(|\lambda_1|,|\lambda_2|)$. If $|\lambda_1|=1$ and $|\lambda_2|<1$, then $\lambda_{1,2}\in\mathbb{R}$. In order to investigate the local bifurcations of the corresponding periodic orbit, we apply center manifold theory to reduce the Poincaré map $\Pi:\Sigma\mapsto\Sigma$ to a one-dimensional map using the method given in [13,31,33]. We first choose a bifurcation parameter among α, β, ω and r, denoted by ζ and fix other parameters. If at the bifurcation value ζ_b, $\lambda_1=\pm1$, then for $|\zeta-\zeta_b|\ll1$, using a center manifold reduction, $\Pi:\Sigma\mapsto\Sigma$ is reduced to a map of the form:

$$w\mapsto p_1(\overline{\zeta})w+p_2(\overline{\zeta})w^2+p_3(\overline{\zeta})w^3+O(|w|^4):=f(\overline{\zeta},w), \tag{4.2}$$

where $w\in\mathbb{R}$ and $\overline{\zeta}:=\zeta-\zeta_b$. If for $\zeta=\zeta_b$, $\lambda_1=-1$, then $p_1(0)=-1$. In this case, if at $(\overline{\zeta},w)=(0,0)$:

$$\eta_1:=\frac{\partial f}{\partial\overline{\zeta}}\frac{\partial^2 f}{\partial w^2}+2\frac{\partial^2 f}{\partial w\partial\overline{\zeta}}\neq0,\quad \eta_2:=\frac{1}{2}\left(\frac{\partial^2 f}{\partial w^2}\right)^2+\frac{1}{3}\frac{\partial^3 f}{\partial w^3}\neq0, \tag{4.3}$$

then the orbit undergoes period doubling bifurcation. Particularly, the bifurcation is supercritical for $\eta_2>0$ and subcritical for $\eta_2<0$. If for $\zeta=\zeta_b$, $\lambda_1=1$, then $p_1(0)=1$. Let

$$q_1:=\frac{\partial^2 f}{\partial w\partial\overline{\zeta}}(0,0),\quad q_2:=\frac{\partial^2 f}{\partial w^2}(0,0),\ q_3:=\frac{\partial^3 f}{\partial w^3}(0,0). \tag{4.4}$$

If $q_1\neq0$ and $q_2\neq0$, then one has transcritical bifurcation. If $q_1\neq0$, $q_2=0$ and $q_3\neq0$, then one has pitchfork bifurcation.

In this section we adopt the same notations as in Sections 2 and 3, and assume that the double impact periodic orbits are not grazing orbits, namely, $\tilde{y}_{m,A}\neq0$ for a $(m,2,0,\mu)$ orbit and $\tilde{y}_{m,B}\neq0$ for a $(m,1,1,\mu)$ orbit. Let

$$F_1^{\pm}(\mu)=1\mp\gamma[2\alpha\omega\sin(2\mu m\pi)+(1+\omega^2)\cos(2\mu m\pi)]c_m \pm\gamma[(1+\omega^2)\sin(2\mu m\pi)-2\alpha\omega\cos(2\mu m\pi)]s_m,$$

$$F_2(\mu)=1-\gamma(1+\omega^2)c_m-2\gamma\alpha\omega s_m.$$

4.1. $(m,2,0,\mu)$ orbits

For a $(m,2,0,\mu)$ orbit, the Poincaré map $\Pi:\Sigma\mapsto\Sigma$ is given by $\Pi=\Pi_2^+\circ\Pi_1^+\circ\Pi_2^+\circ\Pi_1^+$, where $\Pi_1^+:\Sigma\mapsto\Sigma_-^+$ is defined by the impact law (2.2), $\Pi_2^+:\Sigma_-^+\mapsto\Sigma$ is defined by the free-flight motion (2.1). Then $D\Pi=D\Pi_2^+\cdot D\Pi_1^+\cdot D\Pi_2^+\cdot D\Pi_1^+$. Using the implicit differentiation method shown in [5,34], $\mathrm{tr}(D\Pi)$ and $\det(D\Pi)$ evaluated at $(\varphi_m,y_m)\in\Sigma$ that corresponds to a $(m,2,0,\mu)$ orbit are given by

$$\det(D\Pi)=r^4e^{-2\alpha mT},$$

$$\mathrm{Tr}(D\Pi)=\frac{e^{-\alpha mT}}{\Omega^2y_m}\left\{r\Omega\left[2r\Omega\cosh(mT\Omega)-(1+r)\sinh(mT\Omega)\frac{F_1^+(\mu)}{\tilde{y}_{m,A}}\right]y_m +(1+r)\left[(1+r)\sinh((1-\mu)mT\Omega)\sinh(\mu mT\Omega)\frac{F_1^+(\mu)}{\tilde{y}_{m,A}} -r\Omega\sinh(mT\Omega)\right]F_2(\mu)\right\}.$$

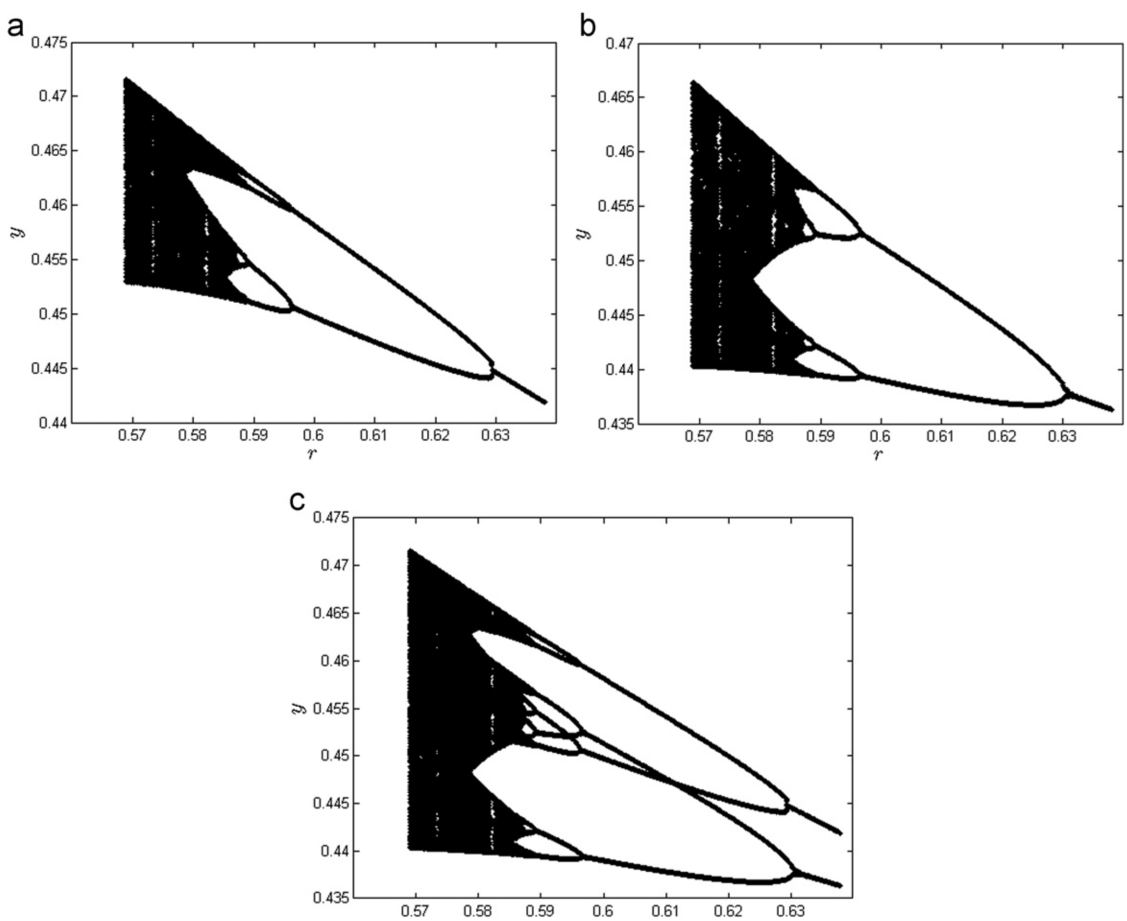

Fig. 6. The period doubling bifurcation diagrams with $\alpha=1.2$, $\omega=4\pi$. (a) For the (3, 2, 0, 0.4) orbit. (b) For the (3, 2, 0, 0.6) orbit. (c) Superposition of (a) and (b).

It is easy to see that $D\Pi$ for the $(m,2,0,\mu)$ orbit and the $(m,2,0,1-\mu)$ orbit have the same determinate and trace. Hence they have the same stability.

For $\alpha>0$ and $r\in(0,1]$, $\det(D\Pi)<1$. Hence a $(m,2,0,\mu)$ orbit cannot undergo Hopf bifurcations. Due to the complexity of computations, it is very difficult to analytically study the bifurcation phenomena of $(m,2,0,\mu)$ orbits when $\max(|\lambda_1|,|\lambda_2|)=1$. Herein we focus our attention on a concrete example using numerical methods.

Take $m=3$, $\alpha=1.2$, $\omega=4\pi$ and $\mu=0.4$ and choose r as bifurcation parameter. By Theorem 2.1 and Corollary 2.1, the (3, 2, 0, 0.4) orbit coexists with the (3,2,0,0.6) orbit when

$$\beta\approx\frac{4.163426513\sqrt{\chi_+(r)}}{r^2+1.970489938r+1.003316548},$$

where $\chi_+(r)=(r^2+1.716809451r+1.056066497)(\ r^2-3.160420784r+3.164381306)$. By direct computation, we find that when $r=r_{pd}^1\approx0.63027619$, $D\Pi$ for the (3, 2, 0, 0.4) orbit and the (3, 2, 0, 0.6) orbit have eigenvalue -1. Apply center manifold theory stated above, we find that in Eqs. (4.2) and (4.3), for the (3, 2, 0, 0.4) orbit, $\eta_1\approx-0.17220137$, $\eta_2\approx54011.5939>0$, and for the (3, 2, 0, 0.6) orbit, $\eta_1\approx-0.17220137$, $\eta_2\approx25977.29826>0$. Thus supercritical period doubling bifurcations of the orbits occur at $r=r_{pd}^1$. Similarly, when $r=r_{tc}^1\approx0.76355112$, $D\Pi$ for the (3, 2, 0, 0.4) orbit and the (3, 2, 0, 0.6) orbit have eigenvalue $+1$. In Eqs. (4.2) and (4.4), for the (3, 2, 0, 0.4) orbit, $q_1\approx-0.1072822$, $q_2\approx-236.7943606$, for the (3, 2, 0, 0.6) orbit, $q_1\approx-0.1072822$, $q_2\approx213.3580012$. Hence the orbits undergo transcritical bifurcation.

To confirm the theoretical bifurcation values $r=r_{pd}^1$ and r_{tc}^1 given above, we present some numerical results as follows.

The period doubling bifurcation diagrams for the (3, 2, 0, 0.4) orbit and the (3, 2, 0, 0.6) orbit are shown in Fig. 6(a) and (b) respectively. From the figures we see that for both orbits, the period doubling cascade leading to chaos when $r\in(0.569,0.638)$. These two bifurcation diagrams are superposed in Fig. 6(c). It is clear from Fig. 6(c) that the chaos attractors of the two orbits interlace with one another.

Fig. 7(a) shows the superposition of the stable branches of the transcritcal bifurcation diagrams for the (3, 2, 0, 0.4) orbit (the lower branch) and the (3, 2, 0, 0.6) orbit (the upper branch). It can be observed that a stable periodic orbit bifurcates from each of these two orbits when $r=r_{tc}^1$, then the stable orbit undergoes period doubling bifurcation at $r\approx0.878$. Fig. 7(b) shows the magnification of (a) for $r\in[0.8640,0.9285]$ and we see the two chaos attractors interlace with one another.

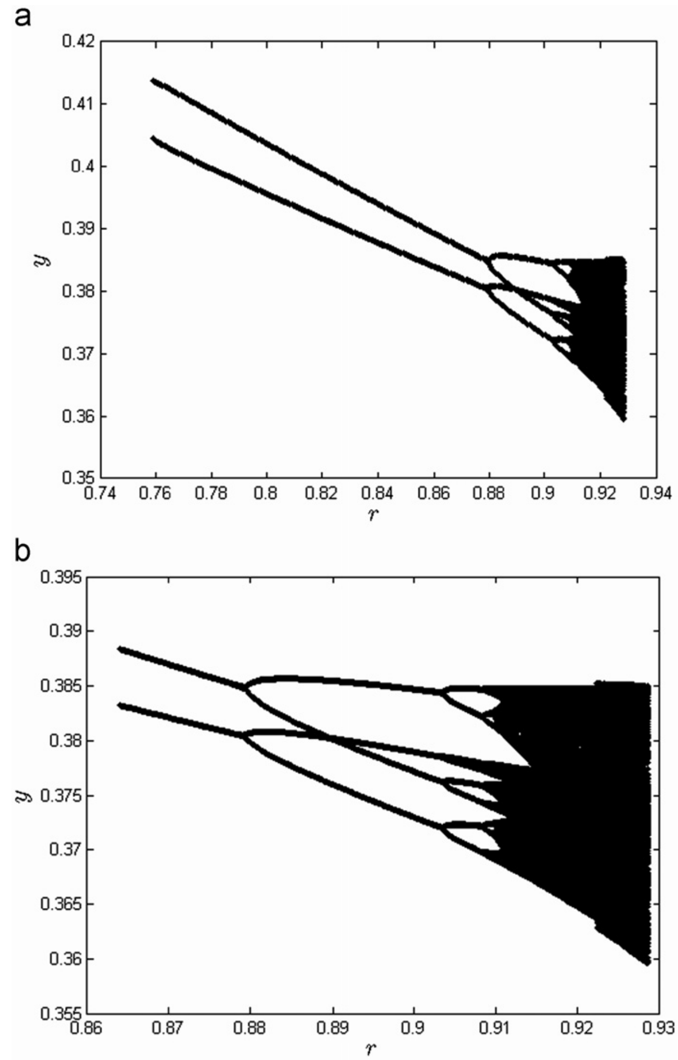

Fig. 7. (a) The transcritical bifurcation diagram for the (3, 2, 0, 0.4) orbit (the lower branch) and the (3, 2, 0, 0.6) orbit (the upper branch) with $\alpha=1.2$, $\omega=4\pi$. (b) Magnification of (a) for $r\in[0.8640,0.9285]$.

4.2. $(m,1,1,\mu)$ orbits

For a $(m,1,1,\mu)$ orbit, the Poincaré map $\Pi:\Sigma\mapsto\Sigma$ is given by $\Pi=\Pi_4^-\circ\Pi_3^-\circ\Pi_2^-\circ\Pi_1^-$, where $\Pi_1^-:\Sigma\mapsto\Sigma_-^+$ and $\Pi_3^-:\Sigma_-^-\mapsto\Sigma_+^-$ are defined by the impact law (2.2), $\Pi_2^-:\Sigma_-^+\mapsto\Sigma_-^-$ and $\Pi_4^-:\Sigma_+^-\mapsto\Sigma$ are defined by the free-flight motion (2.1). Thus $D\Pi=D\Pi_4^-\cdot D\Pi_3^-\cdot D\Pi_2^-\cdot D\Pi_1^-$. $\mathrm{Tr}(D\Pi)$ and $\det(D\Pi)$ evaluated at $(\varphi_m,y_m)\in\Sigma$ that corresponds to a $(m,1,1,\mu)$ orbit are given by

$$\det(D\Pi)=r^4e^{-2\alpha mT},$$

$$\mathrm{Tr}(D\Pi)=\frac{e^{-\alpha mT}}{\Omega^2y_m}\left\{r\Omega\left[2r\Omega\cosh(mT\Omega)+(1+r)\sinh(mT\Omega)\frac{F_1^-(\mu)}{\tilde{y}_{m,B}}\right]y_m\right.$$
$$-(1+r)\left[(1+r)\sinh((1-\mu)mT\Omega)\sinh(\mu mT\Omega)\frac{F_1^-(\mu)}{\tilde{y}_{m,B}}\right.$$
$$\left.\left.+r\Omega\sinh(mT\Omega)\right]F_2(\mu)\right\}.$$

Like for the $(m,2,0,\mu)$ orbit, $D\Pi$ for a $(m,1,1,\mu)$ orbit and a $(m,1,1,1-\mu)$ orbit have the same determinate and trace. Hence they have the same stability. Furthermore, a $(m,1,1,\mu)$ orbit cannot undergo Hopf bifurcations.

In the following we focus on a concrete example to observe the bifurcation phenomena for $(m,1,1,\mu)$ orbits when $\max(|\lambda_1|,|\lambda_2|)=1$.

Take $m=2$, $\alpha=\frac{4}{13}$, $\omega=4\pi$ and $\mu=0.36$. Choose r as bifurcation parameter. By Theorem 2.1 and Corollary 2.1, the (2, 1, 1, 0.36) orbit coexists with the (2, 1, 1, 0.64) orbit when

$$\beta\approx\frac{60.46218915\sqrt{\chi_-(r)}}{r^2+1.979869866r+1.004356884},$$

where $\chi_-(r)=(r^2+1.998745274r+1.000232132)\ (r^2-2.066994008r+1.636537837)$. We find that when $r=r_{pd}^2\approx0.4174924875$, $D\Pi$ for the (2, 1, 1, 0.36) orbit and the (2, 1, 1, 0.64) orbit have eigenvalue -1. We find that in Eqs. (4.2) and (4.3), for the (2, 1, 1, 0.36) orbit, $\eta_1\approx-1.121806$, $\eta_2\approx6688.398819>0$, and for the (2, 1, 1, 0.64) orbit, $\eta_1\approx-1.121806$, $\eta_2\approx252.5065259>0$. Therefore supercritical period doubling bifurcations for the orbits occur. When $r=r_{tc}^2\approx0.4950471839$, $D\Pi$ for the (2, 1, 1, 0.36) orbit and the (2, 1, 1, 0.64) orbit have eigenvalue $+1$. In Eqs. (4.2) and (4.4),

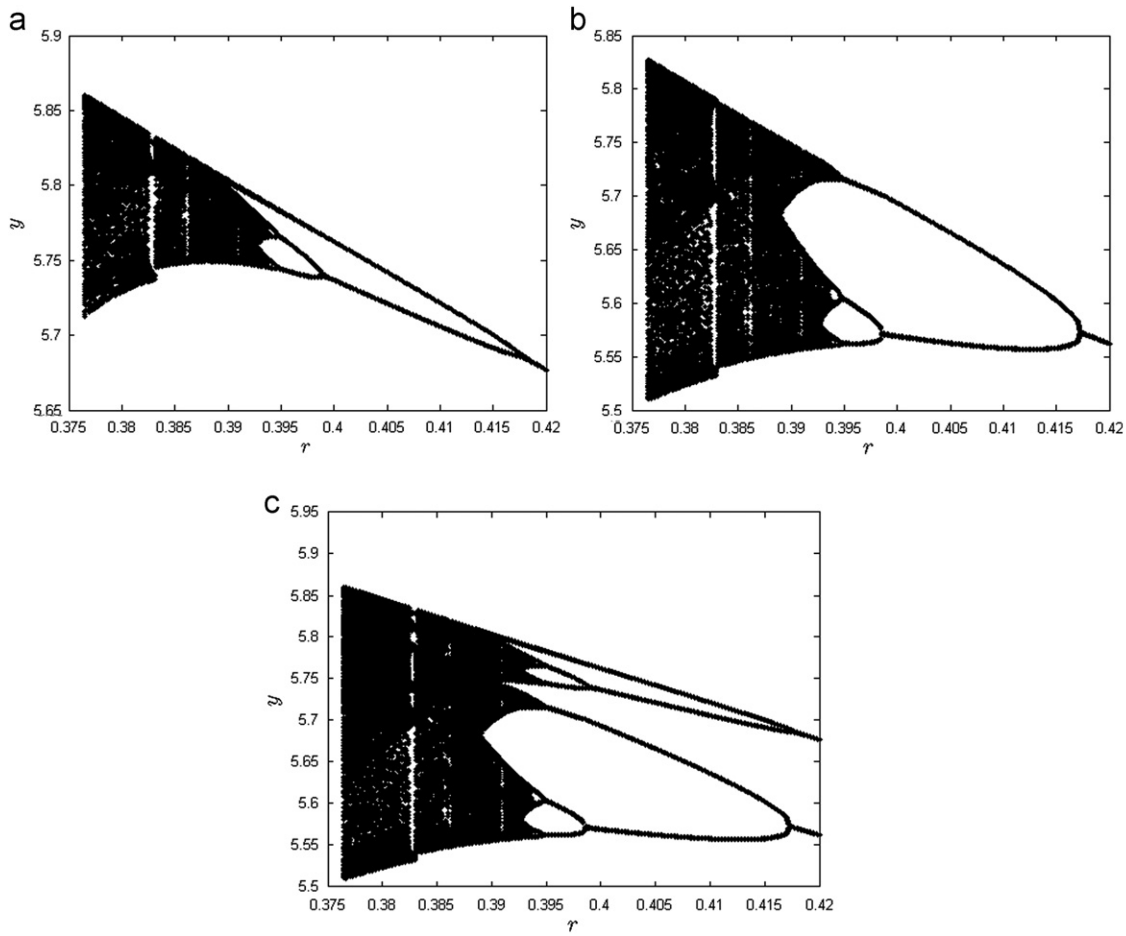

Fig. 8. The period doubling bifurcation diagrams with $\alpha=\frac{4}{13}$, $\omega=4\pi$. (a) For the (2, 1, 1, 0.36) orbit. (b) For the (2, 1, 1, 0.64) orbit. (c) Superposition of (a) and (b).

for the (2, 1, 1, 0.36) orbit, $q_1\approx-0.696589$, $q_2\approx-32.83644736$, for the (2, 1, 1, 0.64) orbit, $q_1\approx-0.696589$, $q_2\approx-40.2364845$. Hence the orbits undergo transcritical bifurcation.

The bifurcation diagrams Fig. 8(a) and (b) show the period doubling cascade leading to chaos for the (2, 1, 1, 0.36) orbit and the (2, 1, 1, 0.64) orbit when $r\in(0.3765,0.4200)$. The two diagrams are superposed in Fig. 8(c). It is clear that the chaos attractors of the two orbits interlace with each other.

The superposition of the stable branches of the transcritcal bifurcation diagrams for the (2, 1, 1, 0.36) orbit (the upper branch) and the (2, 1, 1, 0.64) orbit (the lower branch) is shown in Fig. 9(a). It can be observed that a stable periodic orbit bifurcates from each of these two orbits when $r=r_{tc}^2$, then the stable orbit undergoes period doubling bifurcation at $r\approx0.565$. Fig. 9(b) shows the magnification of (a) for $r\in[0.56,0.59]$ and we see the two chaos attractors interlace with each other.

5. Existence of grazing periodic orbits

In this section we discuss the existence of grazing periodic orbits of system (1.1). With the same notations as in previous sections, as pointed out in Section 2, when $\tilde{y}_{m,A}=0$ (resp. $\tilde{y}_{m,B}=0$), the corresponding $(m,2,0,\mu)$ (resp. $(m,1,1,\mu)$) orbit is a grazing periodic orbit. Let

$$V(\mu)=-e^{\alpha mT}[\alpha Q(1-\mu)+\Omega R(1-\mu)],$$

$$W_\pm(\mu)=\omega[\pm e^{\alpha\mu mT}\sinh(mT\Omega)-e^{\alpha mT}Q(1-\mu)],$$

$$X=I+\frac{\alpha}{\Omega}\sinh(mT\Omega)-\sinh(\alpha mT),$$

$$\Delta_g(\mu)=V(\mu)\sin(2\mu m\pi)-\omega e^{\alpha mT}Q(1-\mu)\cos(2\mu m\pi)+\omega e^{\alpha\mu mT}\sinh(mT\Omega),$$

$$\Delta_{g1}^{\pm}(\mu)=V(\mu)\sin(2\mu m\pi)+W_\pm(\mu)\cos(2\mu m\pi),$$

$$\Delta_{g2}^{\pm}(\mu)=-W_\pm(\mu)\sin(2\mu m\pi)+V(\mu)\cos(2\mu m\pi)\mp V(\mu),$$

$$\Delta_{g3}^{\pm}(\mu)=\frac{\omega}{r}[\Delta_{g2}^{\pm}(\mu)+\Omega e^{\alpha\mu mT}(1\mp\cos(2\mu m\pi))X],$$

$$Z_\pm(\mu)=\Delta_{g2}^{\pm}(\mu)+\frac{\Omega}{1+r}e^{\alpha\mu mT}(1\mp\cos(2\mu m\pi))J.$$

It is easy to see that

$$\begin{aligned}\Delta_g(\mu)&=\Delta_{g1}^{+}(\mu)+\omega e^{\alpha\mu mT}(1-\cos(2\mu m\pi))\sinh(mT\Omega)\\&=\Delta_{g1}^{-}(\mu)+\omega e^{\alpha\mu mT}(1+\cos(2\mu m\pi))\sinh(mT\Omega).\end{aligned}$$

The main result of this section is given as follows.

Theorem 5.1. *Let m be a positive integer and $\mu\in(0,1)$ and $\mu\neq\frac{1}{2}$. Then for system* (1.1):

(1) *A point $(\varphi_m,y_m)\in\Sigma$ is a period-2 point of Π and corresponds to a grazing periodic orbit of type $(m,2,0,\mu)$ if and only if* (2.4d) *and*

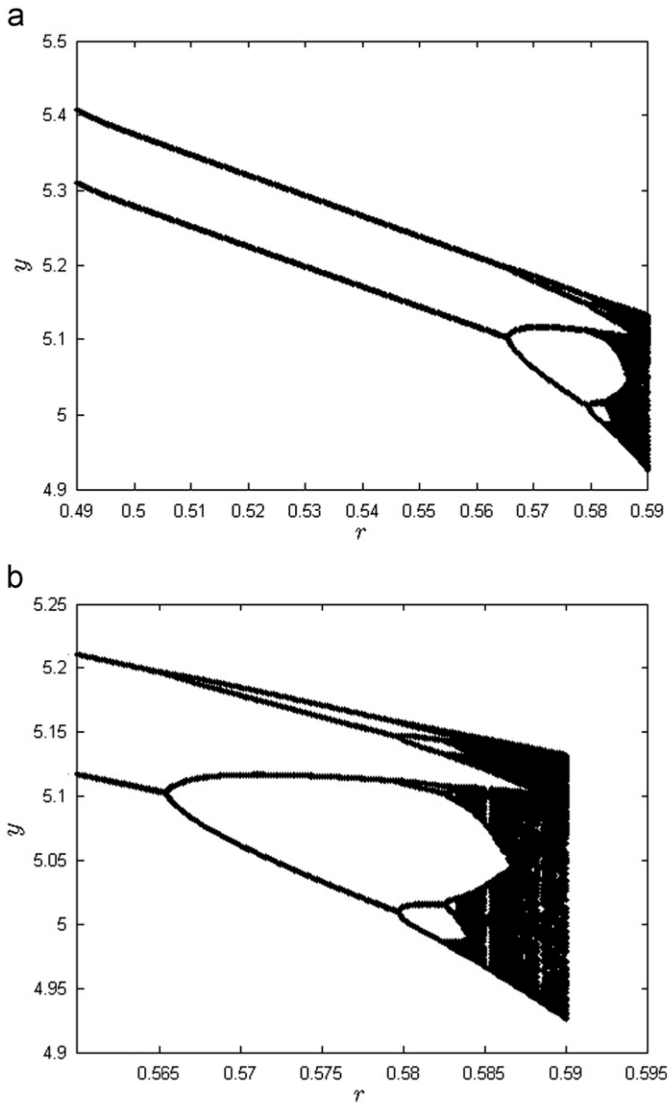

Fig. 9. (a) The transcritical bifurcation diagram for the (2, 1, 1, 0.36) orbit (the upper branch) and the (2, 1, 1, 0.64) orbit (the lower branch) with $\alpha=\frac{4}{13}$, $\omega=4\pi$. (b) Magnification of (a) for $r\in[0.56,0.59]$.

(2.4e) *holds and the following are satisfied*:

$$Z_+(\mu)=0,\quad c_m=\frac{\Delta^+_{g1}(\mu)}{\gamma\Delta_g(\mu)},\quad s_m=\frac{\Delta^+_{g2}(\mu)}{\gamma\Delta_g(\mu)},$$

$$y_m=\frac{\Delta^+_{g3}(\mu)}{\Delta_g(\mu)},\quad \gamma=\frac{\sqrt{\Delta^+_{g1}(\mu)^2+\Delta^+_{g2}(\mu)^2}}{\Delta_g(\mu)}. \tag{5.1}$$

The grazing point is $\mathbf{x}^0=(1,0,\varphi_m+\mu mT)$.

(2) *There is no grazing periodic orbit of type* $(m,1,1,\mu)$.

Proof. (1) We first prove that $\Delta_g(\mu)>0$ for $\mu\in(0,1)$. Let $\mathcal{D}(\mu)=e^{-\alpha\mu mT}\Delta_g(\mu)$. Then

$$\mathcal{D}'(\mu)=mT\sin(2\mu m\pi)e^{\alpha(1-\mu)mT}[(\alpha^2+\Omega^2+\omega^2)Q(1-\mu)+2\alpha\Omega R(1-\mu)].$$

Note that $Q(1-\mu)>0$, we have

$$(\alpha^2+\Omega^2+\omega^2)Q(1-\mu)+2\alpha\Omega R(1-\mu)>2\alpha\Omega[Q(1-\mu)+R(1-\mu)]>0.$$

Hence $\mathcal{D}'(\mu)=0$ if and only if $\sin(2\mu m\pi)=0$, i.e. $\mu=k/2m$ for $k=0,1,\ldots,2m$. These are all of the extreme points of $\mathcal{D}(\mu)$ in [0,1]. It is elementary to prove that $\mathcal{D}(k/2m)>0$ *for* $k=1,\ldots,2m-1$ *and* $\mathcal{D}(0)=\mathcal{D}(1)=0$, implying that $\Delta_g(\mu)>0$.

The results given in (1) can be obtained by solving Eqs. (2.4a)–(2.4c) combined with $\tilde{y}_{m,A}=0$. The expression for $\tilde{y}_{m,A}$ given by (2.6) is used. The details are omitted here for brevity.

(2) We prove the statement by contradiction. If there is a fixed point $(\varphi_m,y_m)\in\Sigma$ of Π that corresponds to a grazing periodic orbit of type $(m,1,1,\mu)$, then similar to (1), we have

$$Z_-(\mu)=0,\quad c_m=\frac{\Delta^-_{g1}(\mu)}{\gamma\Delta_g(\mu)},\quad s_m=\frac{\Delta^-_{g2}(\mu)}{\gamma\Delta_g(\mu)},$$

$$y_m=\frac{\Delta^-_{g3}(\mu)}{\Delta_g(\mu)},\quad \gamma=\frac{\sqrt{\Delta^-_{g1}(\mu)^2+\Delta^-_{g2}(\mu)^2}}{\Delta_g(\mu)}. \tag{5.2}$$

Since for $t\in(0,mT)$, this grazing orbit reaches the wall $x=-1$ after a time μmT with zero approaching velocity and there is no other contact point of the orbit to the impacting walls $x=\pm1$, the orbit can be described by the solution $(x(\varphi_m+t;+1,-ry_m,\varphi_m),y(\varphi_m+t;+1,-ry_m,\varphi_m))$ $(0\le t\le mT)$ of Eq. (2.1). Under the conditions (5.2), we have

$$x(\varphi_m+t;+1,-ry_m,\varphi_m)=1+\frac{\delta(t)}{\Delta_g(\mu)}, \tag{5.3}$$

where

$$\delta(t)=\Delta^-_{g1}(\mu)(\cos\omega t-1)-\Delta^-_{g2}(\mu)\sin\omega t-\omega e^{\alpha(\mu mT-t)}(1+\cos(2\mu m\pi))$$
$$[e^{\alpha t}\sinh(mT\Omega)-e^{\alpha mT}\sinh(\Omega t)-\sinh(\Omega(mT-t))].$$

It is elementary to prove that

$$\delta(t)\ge\sqrt{\Delta^-_{g1}(\mu)^2+\Delta^-_{g2}(\mu)^2}\,\overline{c}_m(t)-[\Delta^-_{g1}(\mu)-(1+\cos(2\mu m\pi))W_-(\mu)],$$

where $\overline{c}_m(t)=\cos(\omega\varphi_m+\psi+\omega t)$. Clearly when $m>1$, or $m=1$ and $c_m=\cos(\omega\varphi_m+\psi)\ne1$, there exists a $t_c\in(0,mT)$ such that $\overline{c}_m(t_c)=1$. Hence

$$\delta(t_c)\ge\sqrt{\Delta^-_{g1}(\mu)^2+\Delta^-_{g2}(\mu)^2}-[\Delta^-_{g1}(\mu)-(1+\cos(2\pi\mu m))W_-(\mu)].$$

On the other hand, for any $\mu\in(0,1)$, we have

$$\Delta^-_{g1}(\mu)^2+\Delta^-_{g2}(\mu)^2-[\Delta^-_{g1}(\mu)-(1+\cos(2\mu m\pi))W_-(\mu)]^2$$
$$=(1+\cos(2\mu m\pi))^2V(\mu)^2\ge0.$$

Thus $\delta(t_c)\ge0$. If $m=1$ and $c_m=1$, then by (5.2), $\Delta^-_{g2}(\mu)=Z_-(\mu)=0$, implying that $\mu=\frac{1}{2}$, which contradicts to the assumption that $\mu\ne\frac{1}{2}$.

Therefore, for any $m\ge1$ and $\mu\in(0,1)$ and $\mu\ne\frac{1}{2}$, there exists a $t_c\in(0,mT)$ such that $\delta(t_c)\ge0$. Since $\Delta_g(\mu)>0$ for $\mu\in[0,1]$ as shown in (1), by (5.3), we have $x(\varphi_m+t_c;+1,-ry_m,\varphi_m)\ge1$, i.e. the pendulum touches the wall $x=+1$ for $t_c\in(0,mT)$. This contradicts to the definition of the $(m,1,1,\mu)$ orbit, implying that there is no grazing periodic orbit of type $(m,1,1,\mu)$. □

It is easy to see that when $m=1$, $\mu=\frac{1}{2}$ and $\beta=q$, there is a corresponding grazing orbit $(x(t;+1,0,\varphi_m),y(t;+1,0,\varphi_m))=(\cos(\omega t+\psi),-\omega\sin(\omega t+\psi))$, but it is not of type $(m,1,1,\mu)$.

Remark 5.1. In order to obtain a grazing orbit of type $(m,2,0,\mu)$, we need to verify that $Z_+(\mu)=0$. Clearly $Z_+(k/m)=0$ for any integer k $(1\le k\le m)$. However, we can prove that for $\mu=k/m$ and $\mu\ne\frac{1}{2}$, (5.1) is not satisfied, implying that grazing orbit of type $(m,2,0,k/m)$ does not exist. In fact, we must use numerical methods to find the zeros of $Z_+(\mu)$ in order to obtain a grazing orbit of type $(m,2,0,\mu)$.

In Fig. 10, take $m=4$, $\alpha=\sqrt{5}$, $r=\frac{1}{3}$, $\omega=2\pi$, we simulate a grazing periodic orbit of type $(4,2,0,\mu)$. Substitute these data into (5.1) we obtain $\mu\approx0.7926290493$, $\beta\approx14.83636873$,

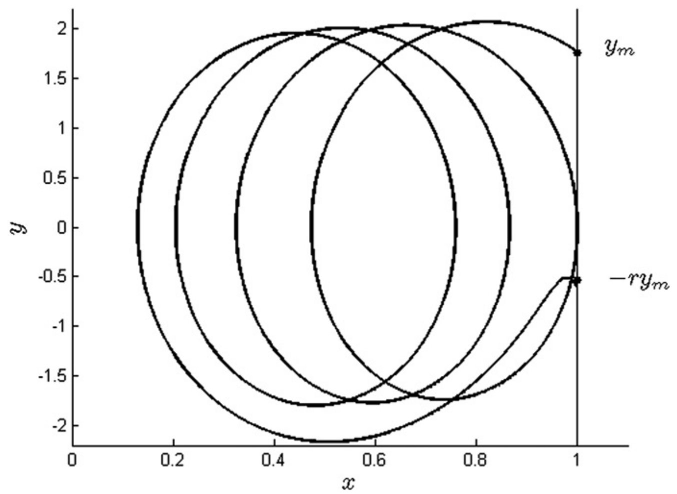

Fig. 10. A grazing periodic orbit of type $(4,2,0,\mu)$ with $m=4$, $\alpha=\sqrt{5}$, $\omega=2\pi$, $r=\frac{1}{3}$.

$\varphi_m \approx 0.2454859631$ and $y_m \approx 1.762324933$. Hence the grazing orbit can be easily plotted.

6. Grazing bifurcations

Let $(\varphi_m, y_m) \in \Sigma$ be a period-2 point of $\Pi : \Sigma \mapsto \Sigma$ that corresponds to a grazing periodic orbit of type $(m,2,0,\mu^0)$ and $\mathbf{x}^0 = (1,0,\varphi_m+\mu^0 mT)$ be the corresponding grazing point. As explained in [2, pp. 261–262], since the Poincaré section Σ is part of the impact surface, the corresponding Poincaré map $\Pi : \Sigma \mapsto \Sigma$ can only describe orbits that intersect Σ. Therefore it is not suitable for analyzing grazing bifurcations. In order to investigate the dynamics near the grazing point $\mathbf{x}^0$, in this section we choose the so-called *normal Poincaré section*:

$$\Sigma_N := \{(x,y,\varphi) \in \mathbb{R} \times \mathbb{R} \times S^1 | y=0\}$$

and construct the normal Poincaré map $\Pi_N : \Sigma_N \mapsto \Sigma_N$ near $\mathbf{x}^0 \in \Sigma_N$. Since the orbits near the grazing orbit intersect with Σ_N transversally, the normal Poincaré map Π_N is well defined. Elements in Σ_N are denoted by $(x,\varphi) \in \mathbb{R} \times S^1$. Under this coordinate system, $\mathbf{x}^0 = (1, \varphi_m + \mu^0 mT) \in \Sigma_N$. Then according to [2, p. 282], $\Pi_N(x,\varphi,\mu) = PDM \circ \tilde{\Pi}_N(x,\varphi,\mu)$ for $(x,\varphi) \in \Sigma_N$ near $\mathbf{x}^0 \in \Sigma_N$ and μ near μ^0, where $PDM : \Sigma_N \mapsto \Sigma_N$ and $\tilde{\Pi}_N : \Sigma_N \mapsto \Sigma_N$ are respectively the *Poincaré discontinuity map* and the *natural Poincaré map* (see [2, Chapter 6] for the definitions of these two maps).

To simplify notations, let

$$\Psi_1(\mu) = \frac{1}{\Omega \Delta_{g3}^+(\mu)}(\Delta_g(\mu) - (1+\omega^2)\Delta_{g1}^+(\mu) - 2\alpha\omega\Delta_{g2}^+(\mu)),$$

$$\Psi_2(\mu) = \cosh(\mu mT\Omega) + \frac{\alpha}{\Omega}\sinh(\mu mT\Omega),$$

$$\Psi_3(\mu) = \omega(W_+(\mu) + \sin(2\mu m\pi)V(\mu)).$$

Let $a^0 = -1 - \beta\cos(\omega\varphi_m + 2\mu^0 m\pi)$, $N(\mu) := (a_{ij}(\mu))_{2\times 2}$ and $M(\mu) := b(\mu)(0,1)^T$, where

$$a_{11}(\mu) = e^{-\alpha mT}[(1+r)\sinh(\mu mT\Omega)\Psi_1(\mu)\Psi_2(1-\mu) - r\Psi_2(1)],$$

$$a_{12}(\mu) = \frac{\omega V(\mu)}{\Delta_g(\mu)}[a_{11}(\mu)-1][1-\cos(2\mu m\pi)] + \frac{(1+r)\omega}{\Delta_g(\mu)}\left\{ e^{-\alpha mT}\frac{\Psi_3(\mu)}{\Omega} \left[\Psi_1(\mu)\sinh(\mu mT\Omega)\sinh((1-\mu)mT\Omega) - \frac{r}{1+r}\sinh(mT\Omega)\right] + e^{-\alpha\mu mT} \left[\omega\frac{\sinh(\mu mT\Omega)}{\Omega}\Delta_{g1}^+(\mu) - (\Psi_1(\mu)\sinh(\mu mT\Omega) - \Psi_2(\mu))\Delta_{g2}^+(\mu)\right]\right\},$$

$$a_{21}(\mu) = \frac{e^{-\alpha mT}(1+r)}{\Omega a^0}\left\{\Psi_1(\mu)\left[\sinh(\mu mT\Omega)\sinh((1-\mu)mT\Omega) + \Omega^2\Psi_2(1-2\mu)\right] - \frac{r}{1+r}\sinh(mT\Omega)\right\},$$

$$a_{22}(\mu) = 1 + \frac{\omega V(\mu)}{\Delta_g(\mu)}[1-\cos(2\mu m\pi)]a_{21}(\mu) + \frac{(1+r)\omega}{a^0\Delta_g(\mu)}\left\{e^{-\alpha mT}\Psi_3(\mu) \left[\Psi_1(\mu)\Psi_2(-\mu)\sinh((1-\mu)mT\Omega) - \frac{r\Psi_2(-1)+e^{\alpha mT}}{1+r}\right] + e^{-\alpha\mu mT} \left[\omega\Psi_2(-\mu)\Delta_{g1}^+(\mu) + \left(\frac{\sinh(\mu mT\Omega)}{\Omega} - \Omega\Psi_1(\mu)\Psi_2(-\mu)\right)\Delta_{g2}^+(\mu)\right]\right\},$$

$$b(\mu) = -\frac{mTe^{-\alpha\mu mT}}{a^0\Delta_g(\mu)}\left\{\left(\frac{\sinh(\mu mT\Omega)}{\Omega} - 2\alpha\Psi_2(-\mu)\right)\left(\omega\Delta_{g2}^+(\mu) - r\Delta_{g3}^+(\mu)\right) + \Psi_2(-\mu)(\Delta_g(\mu) - \Delta_{g1}^+(\mu)) - \omega e^{\alpha\mu mT}\Psi_3(\mu)\right\} - mT.$$

Then using the method given in Chapter 6 of [2], we obtain the following result:

Theorem 6.1. *For system* (1.1), *let* $(\varphi_m, y_m) \in \Sigma$ *be a period-2 point of* $\Pi : \Sigma \mapsto \Sigma$ *that corresponds to a grazing periodic orbit of type* $(m,2,0,\mu^0)$ *and* $\mathbf{x}^0 = (1, \varphi_m + \mu^0 mT) \in \Sigma_N$ *be the corresponding grazing point. For* $\mathbf{x} := (x,\varphi) \in \Sigma_N$ *near* $\mathbf{x}^0$ *and* $\mu \in (0,1)$ *near* μ^0, *let* $\overline{\mathbf{x}} = (\mathbf{x}-\mathbf{x}^0)^T := (\overline{x},\overline{\varphi})^T$ *and* $\overline{\mu} = \mu - \mu^0$. *Then the normal Poincaré map* $\Pi_N : \Sigma_N \mapsto \Sigma_N$ *can be written to leading-order in the form*

$$\Pi_N(\overline{\mathbf{x}},\overline{\mu}) = \begin{cases} N(\mu^0)\overline{\mathbf{x}} + M(\mu^0)\overline{\mu}, & \text{if } \kappa(\overline{\mathbf{x}}) \le 0, \\ N(\mu^0)\overline{\mathbf{x}} + M(\mu^0)\overline{\mu} - (1+r)\sqrt{\dfrac{2\kappa(\overline{\mathbf{x}})}{a^0}}(0,1)^T, & \text{if } \kappa(\overline{\mathbf{x}}) > 0, \end{cases} \tag{6.1}$$

where $\kappa(\overline{\mathbf{x}}) = a_{11}(\mu^0)\overline{x} + a_{12}(\mu^0)\overline{\varphi}$, $a^0 = -1 - \beta\cos(\omega\varphi_m + 2\mu^0 m\pi)$.

By the results of [2, p. 284], we have

Theorem 6.2. *Let the assumptions be given as Theorem* 6.1. *Let* E *be the* 2×2 *unit matrix,* $C = (-1,0)^T$. *Suppose that* $N(\mu^0)$ *has real eigenvalues* $\lambda_{1,2}$ *such that* $0 < \lambda_1 < 1$ *and* $\lambda_2 < \lambda_1$. *Furthermore, suppose that* $\delta_* = C^T(E - N(\mu^0))^{-1}M(\mu^0) \ne 0$ *and* $\zeta_n = C^T N^n(\mu^0)(0,-1)^T > 0$ *for all* $n > 0$. *Then as* $\delta_*(\mu-\mu^0) > 0$ *evolves into* $\delta_*(\mu-\mu^0) < 0$,

(1) *if* $\lambda_1 \in (\frac{2}{3},1)$, *there is a chaotic attractor close to the origin for all small negative values of* $\delta_*(\mu-\mu^0)$;

(2) *if* $\lambda_1 \in (\frac{1}{4},\frac{2}{3})$, *for all small negative values of* $\delta_*(\mu-\mu^0)$, *there is an alternating series of chaotic and stable periodic motions, accumulating in a period-adding cascade as* $\mu \to \mu^0$;

(3) *if* $\lambda_1 \in (0,\frac{1}{4})$, *the chaotic motion disappears and is replaced by periodic bands that overlap and increase in period as* $\mu \to \mu^0$.

In general, it is hard to verify that $\zeta_n > 0$ for all n. In the following we give a simple criterion.

Proposition 6.1. *If* $N(\mu^0)$ *has real eigenvalues* λ_1 *and* λ_2 *such that* $\lambda_1 > \lambda_2$, *then for all* n, ζ_n *has the same sign as* $a_{12}(\mu^0)$.

Proof. Let $p_N(\lambda)$ be the characteristic polynomial of $N(\mu^0)$. By the Hamilton–Cayley theorem, we have $p_N(N(\mu^0)) = 0$. On the other hand, for any n, there is a polynomial $q_n(\lambda)$ such that

$$\lambda^n = q_n(\lambda)p_N(\lambda) + \ell_1\lambda + \ell_2, \tag{6.2}$$

where

$$\ell_1 = \frac{\lambda_1^n - \lambda_2^n}{\lambda_1 - \lambda_2}, \quad \ell_2 = \frac{\lambda_1\lambda_2(\lambda_1^{n-1} - \lambda_2^{n-1})}{\lambda_2 - \lambda_1}.$$

From (6.2) we get $N^n(\mu^0) = \ell_1 N(\mu^0) + \ell_2 E$. Thus $\zeta_n = \ell_1 a_{12}(\mu^0)$ has the same sign as $a_{12}(\mu^0)$ since $\ell_1 > 0$. The proof is complete. □

From the above analysis, it is clear that the matrix $N(\mu^0)$ and the vector $M(\mu^0)$ are important to the investigation of the dynamics of system (1.1) near the grazing point $\mathbf{x}^0$. But their expressions are very complicated. In order to observe the grazing bifurcation phenomena more directly, in the following we use the *Monte Carlo numerical simulation method* described in [2, pp. 115–117], to compute the bifurcation diagrams by varying r, ω, and α each in turn.

(1) Take $m=4$, $\alpha=\sqrt{5}$, $\omega=2\pi$ and vary r from 0.6 to 1. For each fixed r, we apply Theorem 5.1 to find μ^0 and $(\varphi_m,y_m)\in\Sigma$ that correspond to a grazing orbit of type $(m,2,0,\mu^0)$. The results for each of $r=0.6$, 0.8 and 1 are listed in Table 1. The leading eigenvalue λ_1 of $N(\mu^0)$ is also listed. Furthermore, we find that λ_1 increases as r increases and for each fixed r, $a_{12}(\mu^0)>0$ and $\delta_*>0$. From the bifurcation diagrams, Fig. 11, we can clearly see the phenomena described in Theorem 6.2.

(2) Take $m=4$, $\alpha=\sqrt{5}$, $r=\frac{1}{3}$ and vary ω from 4π to 2.8π. Then for each fixed ω, $a_{12}(\mu^0)>0$, $\delta_*>0$ and λ_1 increases as ω increases. In Table 2, for each of $\omega=4\pi$, 3.5π and 2.8π, we list μ^0, $(\varphi_m,y_m)\in\Sigma$ and λ_1 that correspond to a grazing orbit of type $(m,2,0,\mu^0)$. The bifurcation diagrams are shown in Fig. 12.

(3) Take $m=4$, $\omega=\frac{20}{7}\pi$, $r=\frac{1}{3}$ and vary α from $\sqrt{3.3}$ to $\sqrt{5.1}$. Then for each fixed α, $a_{12}(\mu^0)>0$, $\delta_*>0$ and λ_1 decreases as α increases. For each of $\alpha=\sqrt{3.3}$, $\sqrt{3.9}$ and $\sqrt{5.1}$, the values for μ^0, $(\varphi_m,y_m)\in\Sigma$ and λ_1 that correspond to a grazing orbit of type $(m,2,0,\mu^0)$ are listed in Table 3. The bifurcation diagrams are shown in Fig. 13.

7. Concluding remarks

Two types of double impact periodic orbits for an impact inverted pendulum have been studied in detail in this paper. Although the system is piecewise linear, the equations describe the orbits are transcendental and it is impossible to obtain closed form of the

Table 1
$m=4$, $\alpha=\sqrt{5}$ and $\omega=2\pi$.

r	μ^0	φ_m	y_m	λ_1
0.6	0.7998270978	0.2210359996	1.582061169	$0.1255261463\in(0,\frac{1}{4})$
0.8	0.8048909996	0.2041532252	1.459253484	$0.4604937708\in(\frac{1}{4},\frac{2}{3})$
1.0	0.8096781048	0.1884186203	1.349144215	$0.8281814973\in(\frac{2}{3},1)$

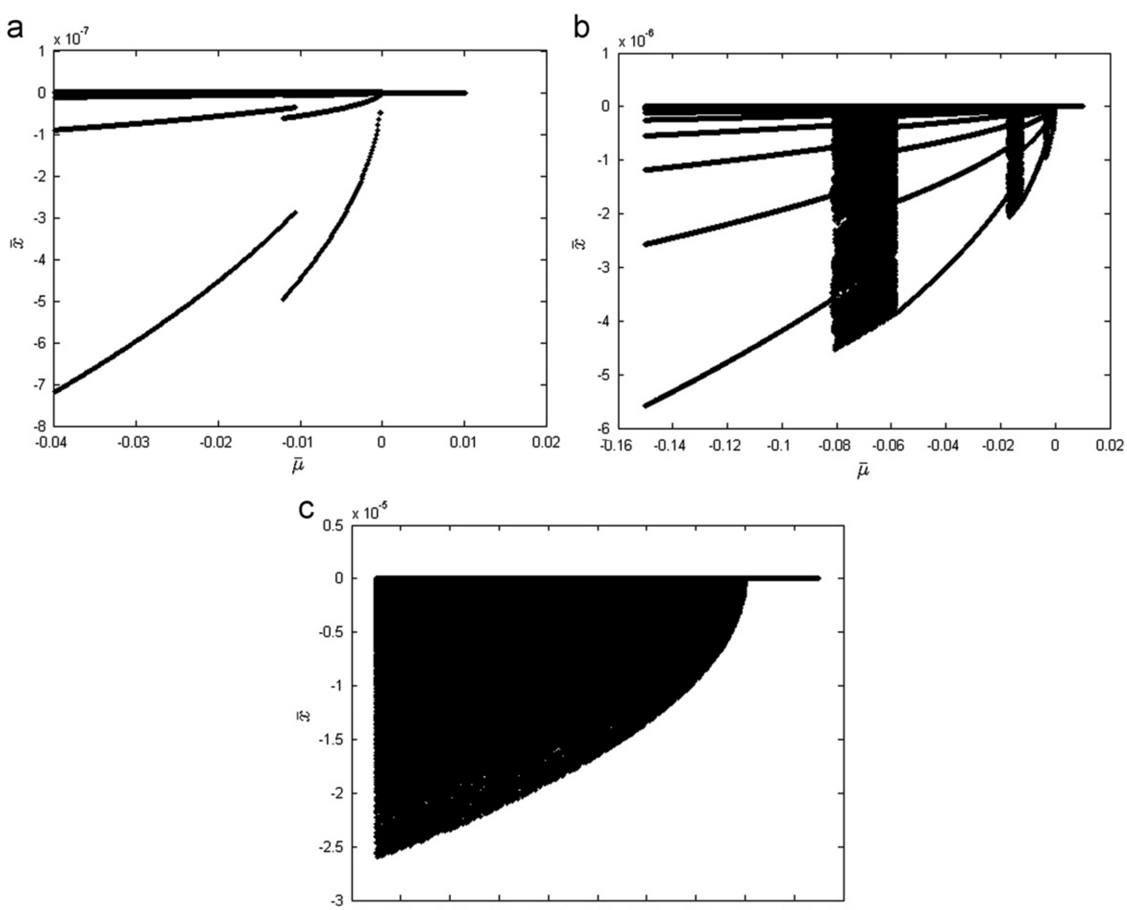

Fig. 11. Bifurcation diagrams in $(\bar{\mu},\bar{x})=(\mu-\mu^0,x-1)$ space for Π_N with $m=4,\alpha=\sqrt{5},\omega=2\pi$; (a) $r=0.6,\mu^0\approx0.7998270978$; (b) $r=0.8,\mu^0\approx0.8048909996$; (c) $r=1$, $\mu^0\approx0.8096781048$.

Table 2
$m=4, \alpha=\sqrt{5}$ and $r=\frac{1}{3}$.

ω	μ^0	φ_m	y_m	λ_1
4π	0.8160321611	0.1056102995	1.266173452	$0.9478542624 \in (\frac{2}{3},1)$
3.5π	0.8108127352	0.1262727208	1.387390066	$0.6097962774 \in (\frac{1}{4},\frac{2}{3})$
2.8π	0.8028005239	0.1671601393	1.577149228	$0.1716002945 \in (0,\frac{1}{4})$

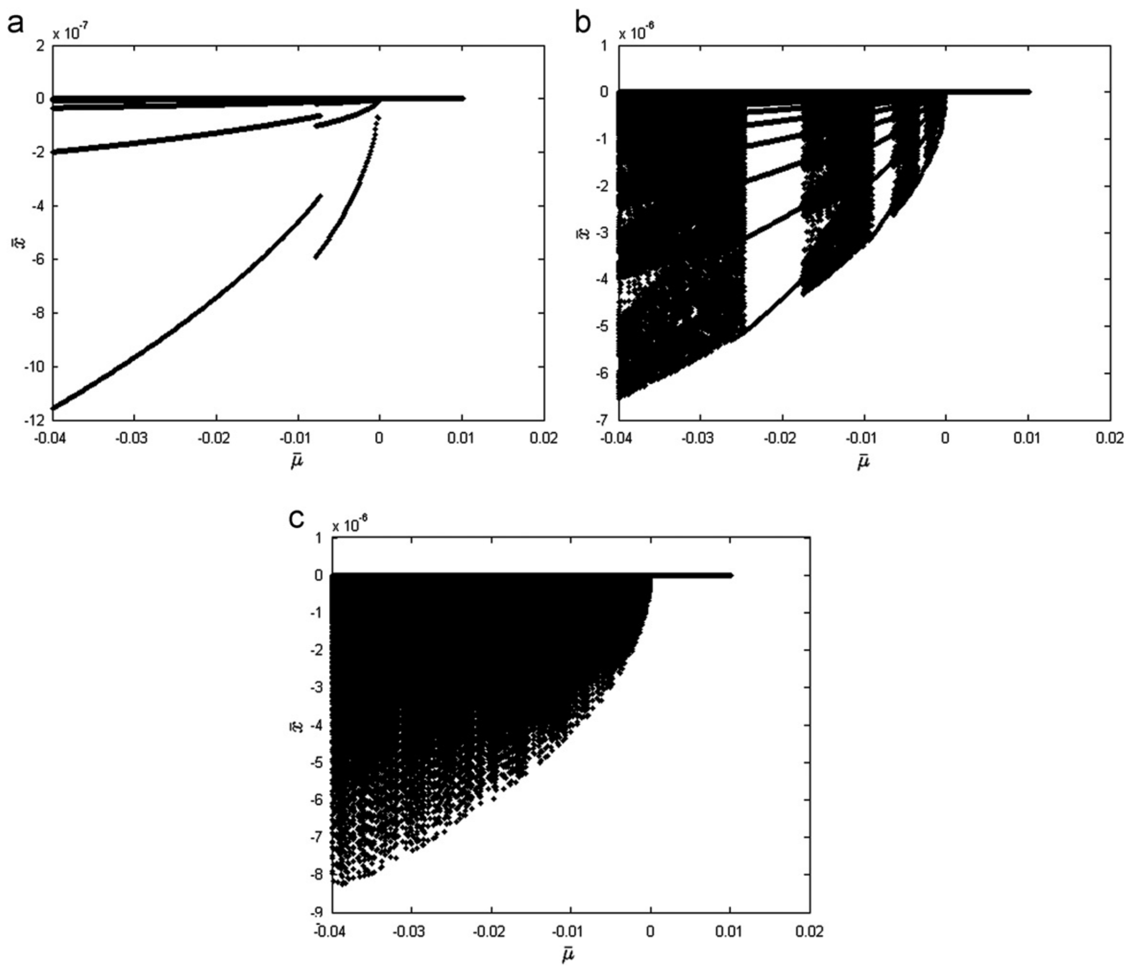

Fig. 12. Bifurcation diagrams in $(\bar{\mu},\bar{x})=(\mu-\mu^0,x-1)$ space for Π_N with $m=4, \alpha=\sqrt{5}, r=\frac{1}{3}$; (a) $\omega=2.8\pi, \mu^0\approx 0.8028005239$; (b) $\omega=3.5\pi, \mu^0\approx 0.8108127352$; (c) $\omega=4\pi, \mu^0\approx 0.8160321611$.

Table 3
$m=4$, $\omega=\frac{20}{7}\pi$ and $r=\frac{1}{3}$.

α	μ^0	φ_m	y_m	λ_1
$\sqrt{3.3}$	0.8130301395	0.1496802316	1.560141371	$0.9746621480 \in (\frac{2}{3},1)$
$\sqrt{3.9}$	0.8091313374	0.1553090275	1.561728126	$0.6230014590 \in (\frac{1}{4},\frac{2}{3})$
$\sqrt{5.1}$	0.8030458715	0.1637033224	1.561107855	$0.1771390216 \in (0,\frac{1}{4})$

corresponding Poincaré maps. Thus we cannot give an exact expressions for the orbits and numerical techniques must be used. From concrete numerical examples, we see that these orbits lose stability through period doubling or transcritical bifurcations. For the double impact periodic orbits that impact at only one of the two walls, grazing bifurcations are also observed. We believe that these results are also true for systems whose free motions between the walls are governed by non-linear equations. However, since the solutions between impacts for non-linear impact systems are generally unknown, perturbation methods must be used.

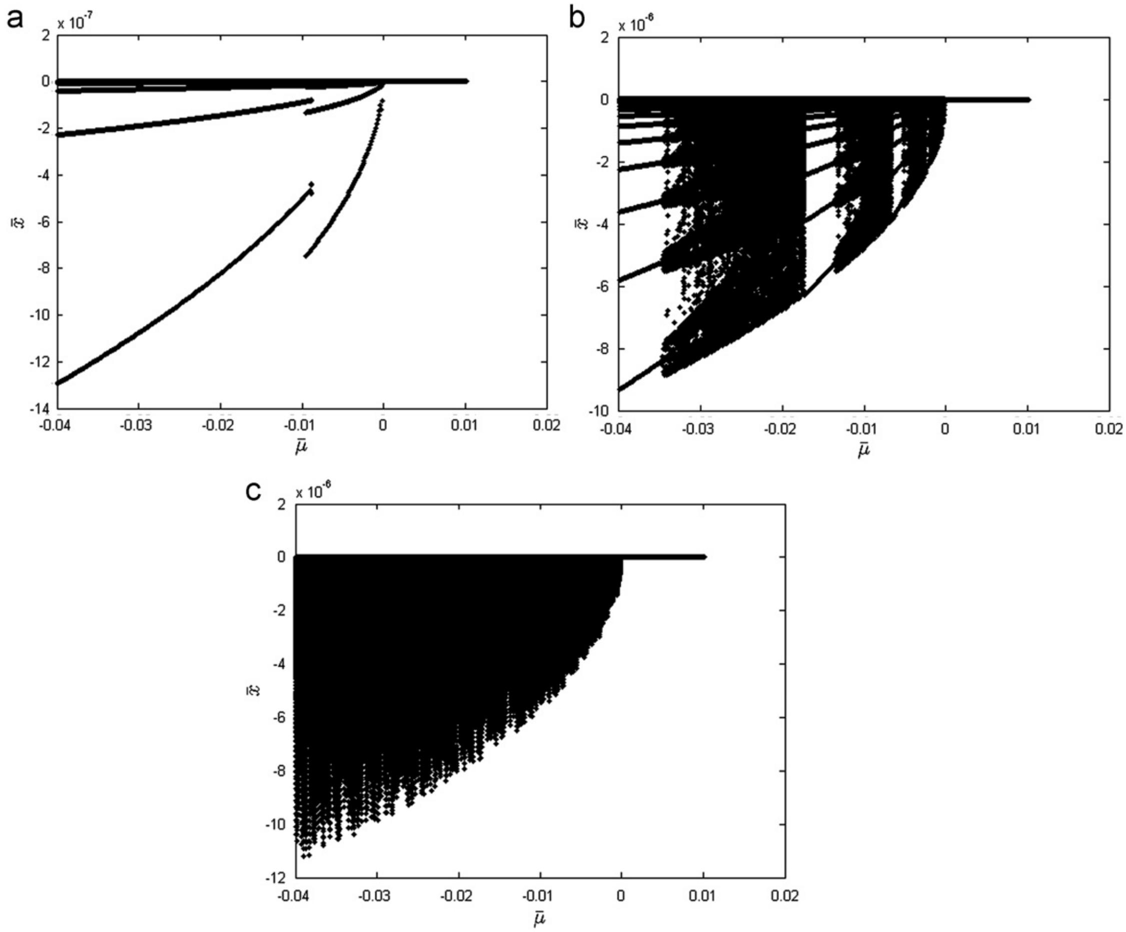

Fig. 13. Bifurcation diagrams in $(\overline{\mu},\overline{x})=(\mu-\mu^0,x-1)$ space for Π_N with $m=4,\omega=\frac{20}{7}\pi,r=\frac{1}{3}$; (a) $\alpha=\sqrt{5.1},\mu^0\approx 0.8030458715$; (b) $\alpha=\sqrt{3.9},\mu^0\approx 0.8091313374$; (c) $\alpha=\sqrt{3.3},\mu^0\approx 0.8130301395$.

References

[1] M.D. Bernardo, C.J. Budd, A.R. Champneys, Normal form maps for grazing bifurcations in n-dimensional piecewise-smooth dynamical systems, Physica D 160 (2001) 222–254.

[2] M.D. Bernardo, C.J. Budd, A.R. Champneys, P. Kowalczyk, Piecewise-Smooth Dynamical Systems: Theory and Applications, Springer-Verlag, London, 2008.

[3] C.J. Budd, A.G. Lee, Double impact orbits of periodically forced impact oscillators, Proc. R. Soc. London A 452 (1996) 2719–2750.

[4] W. Chin, E. Ott, H.E. Nusse, C. Grebogi, Grazing bifurcations in impact oscillators, Phys. Rev. E 50 (1994) 4427–4444.

[5] S.-N. Chow, S.W. Shaw, Bifurcations of subharmonics, J. Differ. Equat. 65 (1986) 304–320.

[6] H. Dankowicz, J. Jerrelind, Control of near-grazing dynamics in impact oscillators, Proc. R. Soc. London Ser. A 461 (2005) 3365–3380.

[7] H. Dankowicz, X. Zhao, Local analysis of co-dimension-one and co-dimension-two grazing bifurcations in impact microactuators, Physica D 202 (2005) 238–257.

[8] L. Demeio, S. Lenci, Asymptotic analysis of chattering oscillations for an impacting inverted pendulum, Q. J. Mech. Appl. Math. 59 (3) (2006) 419–434.

[9] Z. Du, Y. Li, W. Zhang, Type I periodic motions for nonlinear impact oscillators, Nonlinear Anal. Ser. A 67 (2007) 1344–1358.

[10] Z. Du, W. Zhang, Melnikov method for homoclinic bifurcation in nonlinear impact oscillators, Comput. Math. Appl. 50 (2005) 445–458.

[11] S. Foale, S.R. Bishop, Dynamical complexities of forced impacting systems, Philos. Trans. R. Soc. London Ser. A 338 (1992) 547–556.

[12] M.H. Friederiksson, A.B. Nordmark, On normal form calculations in impact oscillators, Proc. R. Soc. London A 456 (2000) 315–329.

[13] J. Guckenheimer, P. Holmes, Nonlinear Oscillations, Dynamical Systems and Bifurcations of Vector Fields, Springer-Verlag, New York, 1983.

[14] F. Hendricks, Bounce and chaotic motion in impact print hammers, IBM J. 27 (1983) 273–280.

[15] S.J. Hogan, On the dynamics of rigid-block motion under harmonic forcing, Proc. R. Soc. London Ser. A 425 (1989) 441–476.

[16] P. Holmes, R.J. Full, D. Koditschek, J. Guckenheimer, Dynamics of legged locomotion: models, analysis and challenges, SIAM Rev. 48 (2006) 207–304.

[20] M. Kunze, Non-Smooth Dynamical Systems, Springer-Verlag, Berlin, Heidelberg, 2000.

[21] S. Lenci, On the suppressions of chaos by means of bounded excitations in an inverted pendulum, SIAM J. Appl. Math. 58 (1998) 1116–1127.

[22] S. Lenci, G. Rega, A procedure for reducing the chaotic response region in an impact mechanical system, Nonlinear Dyn. 15 (1998) 391–409.

[23] S. Lenci, G. Rega, Periodic solutions and bifurcations in an impact inverted pendulum under impulsive excitation, Chaos Solitons Fractals 11 (2000) 2453–2472.

[24] S. Lenci, G. Rega, Regular nonlinear dynamics and bifurcations of an impacting system under general periodic excitation, Nonlinear Dyn. 34 (2003) 249–268.

[25] Y. Li, Z. Du, W. Zhang, Asymmetric type II periodic motions for nonlinear impact oscillators, Nonlinear Anal. Ser. A 68 (2008) 2681–2696.

[26] Y. Ma, J. Ing, S. Banerjee, M. Wiercigroch, E. Pavlovskaia, The nature of the normal form map for soft impacting systems, Int. J. Non-linear Mech. 43 (2008) 504–513.

[27] J. Molenaar, J.G. de Weger, W. van de Water, Mappings of grazing impact oscillators, Nonlinearity 14 (2001) 301–321.

[28] A.B. Nordmark, Non-periodic motion caused by grazing incidence in an impact oscillator, J. Sound Vib. 145 (1991) 279–297.

[29] A.B. Nordmark, Existence of periodic orbits in grazing bifurcations of impacting mechanical oscillators, Nonlinearity 14 (2001) 1517–1542.

[30] E. Pavlovskaia, M. Wiercigroch, Low-dimensional maps for piecewise smooth oscillators, J. Sound Vib. 305 (2007) 750–771.

[31] S.W. Shaw, The dynamics of a harmonically excited system having rigid amplitude constraints, Part 1: subharmonic motions and local bifurcations, J. Appl. Mech. 52 (1985) 453–458.

[32] S.W. Shaw, A.G. Haddow, S.-R. Hsieh, Properties of cross-well chaos in an impacting system, Philos. Trans. R. Soc. London A 347 (1994) 391–410.

[33] S.W. Shaw, P.J. Holmes, A periodically forced piecewise linear oscillator, J. Sound Vib. 90 (1983) 129–155.

[34] S.W. Shaw, R.H. Rand, The transition to chaos in a simple mechanical system, Int. J. Non-linear Mech. 24 (1989) 41–56.

[35] P. Thota, H. Dankowicz, Continuous and discontinuous grazing bifurcations in impacting oscillators, Physica D 214 (2006) 187–197.

[36] P. Thota, H. Dankowicz, Analysis of grazing bifurcations of quasiperiodic system attractors, Physica D 220 (2006) 163–174.